FINAL REPORT

TITLE: X-Ray Microscope Assembly and Alignment Support and Advanced X-Ray Microscope Design and Analysis

PRINCIPAL INVESTIGATOR: David L. Shealy, Ph.D.
Department of Physics
University of Alabama at Birmingham
Campbell Hall, Room 310
Birmingham, AL 35294-1170
205-934-8068
FAX: 205-934-8042
INTERNET: shealy@uabphy.phy.uab.edu

PURCHASE ORDER NO.: H06853D

PERIOD: May 10, 1990 - September 30, 1991

DATE OF PUBLICATION: October 28, 1991

DIST. CODE:
AP29-F (0*)
CN22D (5)
AT01 (1)
CC01/Sheehan (1)
EM (1)
ES52 (5**)
NASA Sci. and Tech. Info. Facility (1 + repro.)
Attn: Accessioning Department
P. O. Box 8757
Baltimore/Washington International Airport, MD 21240

* Copy of letter of transmittal only.
** Copy of letter of transmittal plus copy of Technical Report.
*** Only Unclassified reports.

ABSTRACT

Work under this contract has been focused on two tasks:

1. Advanced x-ray microscope and telescope design, and
2. Assembly and alignment support for Schwarzschild x-ray microscope.

Results obtained as part of Task 1 have been reported to NASA/MSFC PI (R.B. Hoover) and published in Optical Engineering and in the Proceedings of the SPIE. See Appendices 1-3 for reprints of the manuscripts. Work associated with task 2 involved a UAB research assistant (D. Gore) working with R.B. Hoover at NASA/MSFC on this project and developing related technical skills. However, assembly and testing of the Schwarzschild microscope is not complete and is continuing into FY 92, when experimental results are expected.

RESULTS

Some key results of this study are given in Appendix 3 reprint, which reported that an aspherical Head microscope could obtain an object plane resolution of 50 Å when operating with 40 Å radiation at NA=0.4. For a magnification of 40x and secondary vertex radius of curvature of 5 cm, this Head microscope will enable recording diffraction limited resolution on film with a grain size of 2,000 lp/mm. For this microscope configuration, one determines from Table I of Appendix 1 that the object-to-image distance is about 1.5 m, which is manufacturable. With a smaller secondary radius of curvature, the total system length can further be reduced.

The major conclusion of this design study is to determine if microscope substrate fabrication technology is capable of making and testing a large NA Head microscope. This technology development is necessary to achieve the 100 Å resolution goal of the Water Window X-Ray Microscope, summarized in Appendix 2. Furthermore, while work is in progress on substrate fabrication of a Head microscope, it is recommended that an independent effort be directed towards 40 Å multilayer reflectivity performance enhancement.

APPENDIX 1

"Design and analysis of aspherical multilayer imaging x-ray microscope"

David L. Shealy and Richard B. Hoover

Optical Engineering, Vol. 30 No. 8, 1094-1099, (1991)

Design and analysis of aspherical multilayer imaging x-ray microscope

David L. Shealy, MEMBER SPIE
Wu Jiang, MEMBER SPIE
University of Alabama at Birmingham
Department of Physics
Birmingham, Alabama 35294

Richard B. Hoover, MEMBER SPIE
NASA Marshall Space Flight Center
Space Science Laboratory
Huntsville, Alabama 35812

Abstract. Considerable effort has been devoted recently to the design, analysis, fabrication, and testing of spherical Schwarzschild microscopes for soft x-ray applications in microscopy and projection lithography. The spherical Schwarzschild microscope consists of two concentric spherical mirrors configured such that the third-order spherical aberration and coma are zero. Because multilayers are used on the mirror substrates for soft x-ray applications, it is desirable to have a small number of reflecting surfaces in the microscope. In order to reduce the microscope aberrations and increase the field of view, generalized mirror surface profiles have been considered in this study for a two-mirror microscope. Based on incoherent, sine wave modulation transfer function (MTF) calculations, the object plane resolution of a 20× microscope has been analyzed as a function of the object height and numerical aperture (NA) of the primary for several spherical Schwarzschild, conic, and aspherical reflecting two-mirror microscope configurations. The ultimate resolution of an aspherical, two-mirror microscope appears to be about 200 Å when using 100-Å radiation. Better resolution can be achieved when shorter wavelength radiation is used.

Subject terms: x-ray/EUV optics; x-ray microscopes; multilayers; Schwarzschild objective.

Optical Engineering 30(8), 1094-1099 (August 1991).

CONTENTS

1. INTRODUCTION

Recent experiments by several groups[1-5] have demonstrated that the Schwarzschild configuration of a reflecting microscope (see Fig. 1) will produce high resolution soft x-ray images. A minimum feature size less than 0.1 μm has been reported,[5] when using 130-Å radiation from a synchrotron for projection lithography applications. Several design studies[6-8] have predicted that a spherical Schwarzschild configuration would be able to produce images with this level of spatial resolution. Because the spherical Schwarzschild microscope has only been corrected for third-order spherical aberration and coma, these microscopes achieve their best resolution when used with a small NA in the range of 0.1 to 0.14, as illustrated in Fig. 2 for an on-axis source point. For larger NA, the aberrations of a spherical Schwarzschild microscope degrade image resolution significantly.

In this paper, the advantages of using an aspherical two-mirror microscope will be explored. Some years ago, Head[9] presented an analytical solution for the differential equations of the aspherical two-mirror microscope in the general configuration shown in Fig. 1, where both the Abbe Sine Condition and the constant optical path length condition are rigorously satisfied for all rays. Until recently, the technology was not available to construct general aspherical surfaces with sufficient surface smoothness to be useful in multilayer x-ray optics applications. During the development of the optics for the Multi-Spectral Solar Telescope Array (MSSTA),[10] it was established that the advanced flow polishing[11] method permits the fabrication of ultrasmooth and precisely figured conic mirror surfaces. Mirrors with rms surface roughness ranging from 0.5 Å to 2 Å rms have been fabricated.

The advanced flow polishing methods utilized by Baker Consulting[11] in the fabrication of these optics permitted the production of ultrasmooth surfaces on the hyperboloidal primary and secondary optical elements while allowing the mirror figure to be closely monitored. Interferometric measurements were taken during the fabrication process, and great care was taken to control the midrange spatial frequency errors. These errors play a significant role in determining the size and shape of the central core of the image and may significantly affect the resultant resolution.

The role of the spatial frequency errors on system resolution has been discussed by Zmek et al.[12] and Harvey et al.[13] In another study, Spiller et al.[14] have discussed the contributions of the roughness and figure errors from different spatial frequency ranges in the power spectral density of their 10-in.-diam rocket mirror. Walker et al.[15] have discussed the diverse factors affecting the final resolution obtainable with the flight MSSTA Ritchey-Chrétien telescopes and have concluded that for some of the extreme ultraviolet (EUV) telescopes operating in spectral

Invited paper XR-107 received Jan. 29, 1991; revised manuscript received March 12, 1991; accepted for publication March 13, 1991.

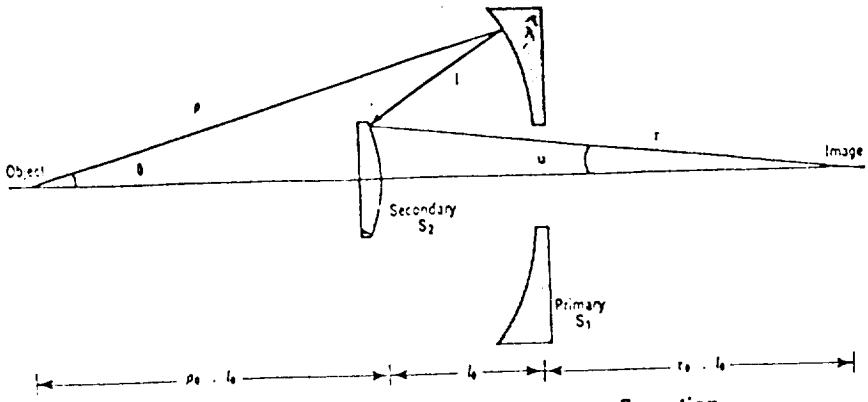

Fig. 1. Generalized two-mirror microscope configuration.

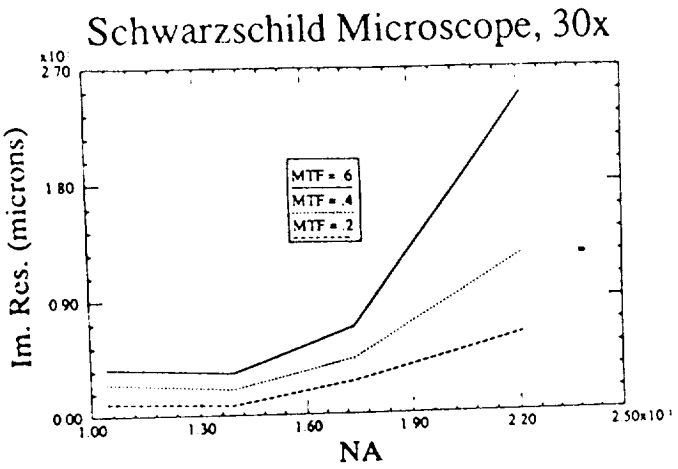

Fig. 2. Image plane resolution of a spherical reflecting microscope for MTF = 20, 40, and 60% as a function of primary mirror NA for 100-Å radiation. Note that the object plane resolution is equal to the image plane resolution divided by the magnification.

lines with adequate solar flux (e.g., 173 Å, 304 Å) spatial resolution of 0.1 arcsec may be achieved. Hoover et al.[16,17] have interferometrically tested the assembled and aligned Ritchey-Chrétien optical systems and found the system rms wavefront errors of the MSSTA telescopes to be less than $\lambda/100$ when tested with a Zygo interferometer operating at a wavelength of 6328 Å.

The resolution of the normal incidence multilayer imaging aspheric x-ray microscope is subject to the same types of factors considered by Walker et al.,[15] with the exception of course of those contributions unique to an instrument on a rocket pointing system (e.g., image blurring caused by pointer jitter and tracking errors), which are not relevant for a ground-based x-ray microscope. However, blur caused by source motion could be a factor for investigations in which living cells are being imaged.

The experience that we have gained in the fabrication, optical alignment, interferometric, visible light, and x-ray investigations of the performance and characteristics of the MSSTA telescopes have led us to conclude that the technology currently exists that is required for the production of normal incidence multilayer optics of spherical configurations (Schwarzschild systems) and of conic or aspheric configurations (Head systems).

Hence, we have decided to examine the optical performance of the Head and several other conic and aspherical two-mirror microscope configurations and to determine when aspherical surfaces can be justified for use in a normal incidence x-ray microscope. In the next section, a summary of the Head microscope equations[9] are presented, and efforts to fit these mirror surface profiles to conventional aspherical surface equations, which are used in optical design, are discussed.

2. ASPHERICAL REFLECTING MICROSCOPE SURFACES

In order to improve the optical performance of a third-order design, such as the spherical Schwarzschild microscope,[7] one often seeks an optical system that rigorously satisfies for all rays both the Abbe Sine Condition:

$$\sin\theta = m \sin u \ , \tag{1}$$

and the constant optical path length condition of axial stigmatism:

$$\rho + r + l = \rho_0 + r_0 + l_0 \tag{2}$$

where m is the microscope magnification, and the variables (ρ, r, l) are defined in Fig. 1. The constants (ρ_0, r_0, l_0) are the paraxial values of the corresponding variables and are illustrated in Fig. 1. This type of microscope is called an aplanat, which is free of all orders of spherical aberration and coma. In 1957, Head[9] presented an analytical solution in finite form for a two-mirror aplanat working between finite foci, i.e., a microscope or projection system. The primary and secondary mirror surfaces are specified by the following equations:

Primary microscope mirror

$$\frac{l_0}{\rho} = \frac{(1+\kappa)}{2\kappa} + \frac{(1-\kappa)}{2\kappa}\cos\theta + \left(\frac{l_0}{\rho_0} - \frac{1}{\kappa}\right)\left(\frac{\gamma}{1+m}\right)^{-1} * \left[\frac{\gamma-(1-m)}{2m}\right]^{\alpha}\left[\frac{\gamma-(m-1)}{2}\right]^{\beta} * \left|\frac{(\kappa+1)\gamma}{(2m+2)} - \frac{(\kappa-1)}{2}\right|^{2-\alpha-\beta} , \tag{3}$$

where $\kappa = (\rho_0 + r_0)/l_0$, $\alpha = m\kappa/(m\kappa - 1)$, $\beta = m/(m - \kappa)$, and $\gamma = \cos\theta + [(m^2 - \sin^2\theta)]^{1/2}$.

Secondary microscope mirror

$$\frac{l_0}{r} = \frac{(1+\kappa)}{2\kappa} + \frac{(1-\kappa)}{2\kappa}\cos u + \left(\frac{l_0}{r_0} - \frac{1}{\kappa}\right)\left(\frac{\delta}{1+M}\right)^{-1} * \left[\frac{\delta - (1-M)}{2M}\right]^{\alpha'} \left[\frac{\delta - (M-1)}{2}\right]^{\beta'} * \left|\frac{(\kappa+1)\delta}{(2M+2)} - \frac{(\kappa-1)}{2}\right|^{2-\alpha'-\beta'}, \quad (4)$$

where $M = 1/m$, $\alpha' = M\kappa/(M\kappa - 1)$, $\beta' = M/(M-\kappa)$, and $\delta = \cos u + [(M^2 - \sin^2 u)]^{1/2} = M\gamma$. Chase[18] noted that absolute value signs should have been added to the original Head equations, Eqs. (3) and (4), to permit a wider application of these equations to the Wolter type I grazing incidence microscope configuration. Chase[18] also presents an interesting comparison between Head and Wolter type I (ellipsoid-hyperboloid) microscope performance.

For paraxial rays, the vertex radii of curvature of the primary and secondary microscope mirrors reduce to

$$R_1 = \frac{2ml_0\rho_0}{m(\rho_0 + l_0) - r_0}, \quad (5)$$

$$R_2 = \frac{2l_0 r_0}{r_0 + l_0 - m\rho_0}. \quad (6)$$

For the same input parameters m, r_0, l_0, and ρ_0, Eqs. (5) and (6) predict the spherical Schwarzschild mirror radii in agreement with values given in Table 1 for magnifications ranging from 10 to 50×.

It is straightforward to evaluate the mirror surface profiles of a Head microscope for given input parameters (m, r_0, l_0, and ρ_0) from Eqs. (3) and (4). In order to use a conventional optical design program to analyze the performance of a Head microscope, it is necessary to fit an equation to the numerical data representing the primary and secondary mirror surfaces of the Head microscope.

Initially, consider that the Head mirror surfaces can be represented by a conic term plus aspherical contributions in the form

$$z(h) = \frac{c\,h^2}{1 + [1 - (k+1)\,c^2\,h^2]^{1/2}} + dh^4 + eh^6 + fh^8. \quad (7)$$

where the curvature $c = 1/R$, h is the height of a ray from the optical axis, k is the conic constant, and (d, e, f) are the aspherical coefficients. (Higher order aspherical terms as well as odd powers in h can be considered but were not in this study.) The vertex radius of curvature R for the Head primary and secondary surfaces are given by Eqs. (5) and (6). The aspherical coefficients have been determined by minimizing the least squared deviation between the surface data points (h_i, z_i) computed from Eqs. (3) and (4) and the fitted data points (h_i, $z(h_i)$) computed from Eq. (7). The conic constants cannot readily be evaluated by a linear least-squares technique. By random variation of the conic constant such that the least-squared error between the Head surface data and the fit data is minimized, an initial set of surface parameters for the Head microscope is determined. Further optimization of the conic constants of the Head microscope has been performed by minimizing an optical design merit function.

Table 1. Schwarzschild mirror parameters.

M(×)	R_1(cm)	R_2(cm)	$\rho_0 - l_0$ (cm)	l_0(cm)	$r_0 - l_0$ (cm)	f(cm)
2	108.00	10.00	18.25	98.00	−91.42	5.51
3	58.27	10.00	18.05	48.27	−34.12	6.04
4	45.58	10.00	18.01	35.58	−13.56	6.41
5	40.00	10.00	18.00	30.00	0.0	6.67
10	31.79	10.00	18.02	21.79	48.36	7.29
15	29.69	10.00	18.04	19.69	91.04	7.54
20	28.75	10.00	18.05	18.75	131.49	7.67
30	27.84	10.00	18.06	17.84	213.27	7.80
40	27.40	10.00	18.07	17.40	296.07	7.87
50	27.15	10.00	18.07	17.15	376.42	7.92

Several optical design merit functions can be used. First, one can vary surface parameters to force all rays to have constant optical path length (zero spherical aberration) and/or to require the Abbe Sine Condition to be satisfied (zero coma). Also, one could optimize the rms blur circle, the FWHM of the point spread function, some combination of third- and fifth-order aberration coefficients, or some feature of the MTF. However, it is very difficult to reduce field curvature in addition to spherical aberration and coma for this configuration of a reflecting microscope. The object plane resolution of a spherical versus aspherical 20× microscope has been analyzed as a function of primary NA and object height for 100 Å radiation. Also, the conic constants of both microscope mirrors have been varied to find a system with zero spherical aberration and coma, based on third- and fifth-order aberration theory.

3. RESULTS

An earlier study[8] of the performance of a spherical Schwarzschild microscope reported that the image plane resolution for an on-axis source was a linear function of the magnification with the slope depending on the value of the MTF used to establish a specified level of resolution. The present analysis has only considered the performance of 20× microscopes. The 20× spherical Schwarzschild microscope whose parameters are given in Table 2 was used as a reference system for comparison with an optimized Head microscope such that the third- plus fifth-order spherical aberration is zero. As we shall see, these systems have very good on-axis resolution. Figure 3 presents a comparison between the performance of a 20× spherical Schwarzschild and aspherical microscope for different values of the MTF. Specifically, the object plane resolution is plotted as a function of the NA of the primary for an on-axis source point. From these results, it follows that for NA less than 0.18, the spherical Schwarzschild and aspherical systems have similar on-axis performance. However, for larger NA, the aspherical microscope has significantly better object plane resolution. From the MTF = 20% plot, it follows that for NA = 0.225, an ultimate resolution of 200 Å can be produced by an aspherical two-mirror microscope over a small field of view using 100-Å radiation. A

Table 2. Schwarzschild microscope system parameters.

Magnification	20x
Focal Length	6.133 cm
Primary Mirror	
Radius of Curvature	23.0 cm
Outside Diameter	8.0 cm
Hole Diameter	2.2 cm
Secondary Mirror	
Radius of Curvature	8.0 cm
Outside Diameter	2.0 cm
Object Distance from Secondary	14.44 cm
Mirror Spacing	15.0 cm
Image Distance from Primary	105.19 cm
Overall Length	134.53 cm

better resolution will result when shorter wavelength radiation is used; however, optimal matching of detector resolution to these small image plane resolution elements may require larger system magnification and lengths. Some aspherical microscope surface parameters for different NA are given in Table 3.

Figure 4 compares the object plane resolution of the spherical Schwarzschild and aspherical microscope as a function of object height for NA = 0.20. Clearly, the aspherical system has better performance for object heights less than 0.3 mm, which is due to the specific merit function used for the optimization. Similar trends hold for other values of the MTF. Figure 5 compares the object plane resolution of the spherical Schwarzschild and aspherical microscope as a function of object height for NA = 0.27. In this case, the aspherical system has better object plane resolution than the spherical Schwarzschild system for heights less than 0.6 mm with similar results for other values of the MTF.

Table 3. Aspherical microscope parameters (20 ×).

R_1 = −22.98 cm; $d = -0.6828\times10^{-12}$; $e = 0.3413\times10^{-16}$; $f = 0.1488\times10^{-21}$

R_2 = −7.95 cm; $d = -0.3509\times10^{-9}$; $e = 0.5400\times10^{-13}$; $f = -0.1114\times10^{-16}$

Mirror Spacing (l_0) = 15.00 cm

Object Distance from Secondary Vertex ($\rho_0 - l_0$) = 14.44 cm

Image Distance from Primary Vertex ($r_0 - l_0$)

NA	0.05	0.13	0.20	0.27
k_1	−0.00064	−0.000599	−0.0005354	−0.000427
k_2	−0.00523	−0.00523	−0.00523	−0.00523
D_1 (cm)	3.00	7.76	12.0	16.4
d_1 (cm)	0.7	1.80	3.0	4.0
D_2 (cm)	0.6	1.6	2.4	3.6
(r_0-l_0) (cm)	105.25	105.24	105.22	105.15

D_1 = Outside Diameter of Primary

d_1 = Hole Diameter of Primary

D_2 = Outside Diameter of Secondary

k_1, k_2 = Conic Constants of the Primary and Secondary

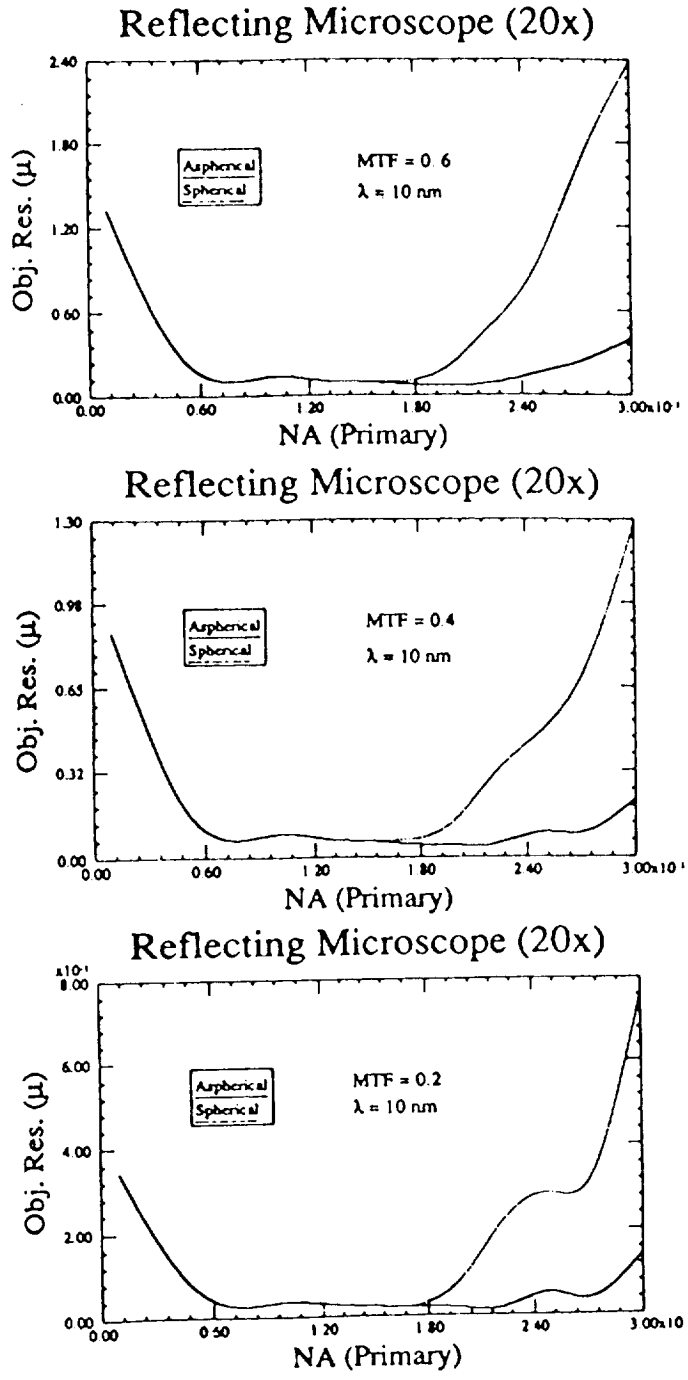

Fig. 3. Comparison of object plane resolution between spherical and aspherical microscope as a function of primary mirror NA.

For all of these systems (both spherical Schwarzschild and aspherical microscope), the third-order field curvature is an important aberration that limits the field of view and appears not to be affected by these optimizations. The magnitude of the field curvature for a 0.5-mm, off-axis source point ranges from 0.1 μm for NA = 0.13 to 0.3 μm for NA = 0.27. Also, the astigmatism and distortion are both very small for these configurations.

Additional optimization of the aspherical microscope was conducted by varying both conic constants in search of a system that simultaneously had both zero third- plus fifth-order coma and spherical aberration. Figure 6 presents the results of this optimization. However, the system identified by the intersection

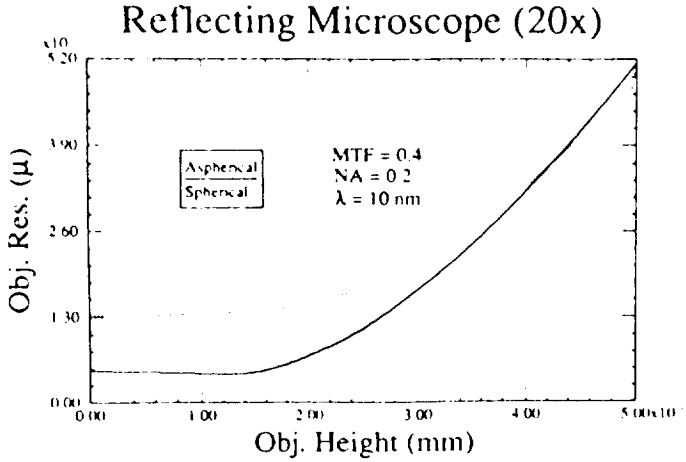

Fig. 4. Comparison of the object plane resolution as a function of object height for primary mirror NA = 0.2.

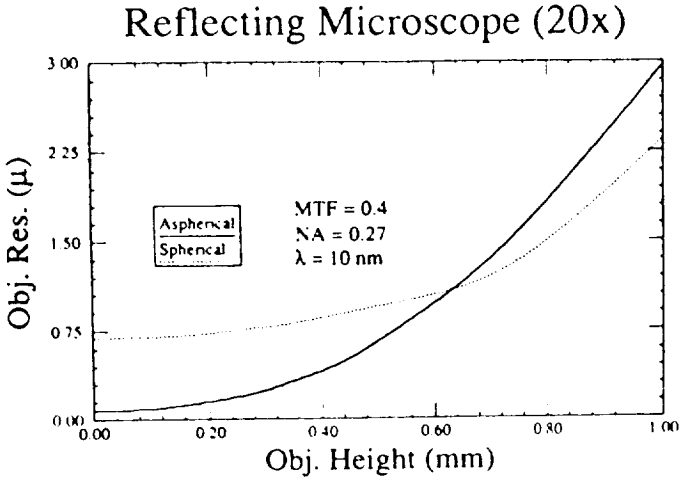

Fig. 5. Comparison of the object plane resolution as a function of object height for primary mirror NA = 0.27.

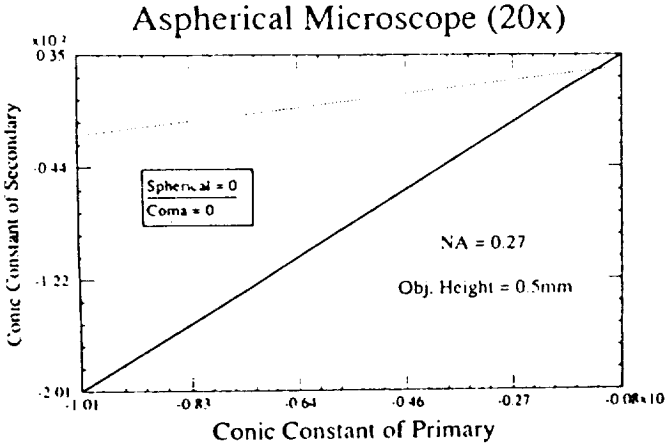

Fig. 6. Conic constants of secondary versus primary mirrors of aspherical microscope systems with zero spherical aberration and coma.

of the two straight lines with zero coma and spherical aberration does not have significantly improved optical performance when compared to the systems described in Table 3. In order to increase the field of view, it will be necessary to use another mirror in the system or to consider generalized mirror surfaces not described by Eq. (7).

4. CONCLUSIONS

Based on these calculations, it has been shown that aspherical microscopes offer higher resolution than spherical systems for NA greater than 0.18. With further optimization of the aspherical microscopes described in Table 3, it has been shown that similar performance can be achieved with a two-mirror conic microscope, without considering the aspherical terms. The ultimate resolution of the aspherical two-mirror microscope with NA = 0.225 appears to be 200 Å over a small field of view with 100-Å radiation where the magnification will need to be adjusted to match detector resolution limits. For larger fields of view, it will be necessary to use additional mirrors to achieve resolution less than 0.1 μm.

5. ACKNOWLEDGMENTS

The authors would like to express gratitude to the Center Director's Discretionary Fund of NASA/MSFC for partial support of this research.

6. REFERENCES

1. H. Kinoshito, K. Kurilhara, Y. Ishil, and Y. Torii, "Soft x-ray reduction lithography using multilayer mirrors," J. Vac. Soc. Technol. B7(6), 1648–1651 (1989).
2. K. A. Tanaka, M. Kado, H. Daido, T. Yamanaka, S. Nakai, K. Yamashita, and S. Kitamoto, "Schwarzschild microscope at λ = 7 nm," in *Soft-X-Ray Projection Lithography, 1991*, Technical Digest Series, Optical Society of America, Washington, DC, pp. 77–79 (1991).
3. D. W. Berreman, J. E. Bjorkholm, L. Eichner, R. R. Freeman, T. E. Jewell, W. M. Mansfield, A. A. MacDowell, M. L. O'Malley, E. L. Raab, W. T. Silfvast, L. H. Szeto, D. M. Tennant, W. K. Waskiewicz, D. L. White, D. L. Windt, O. R. Wood II, and J. H. Bruning, "Soft-x-ray projection lithography: printing of 0.2-μm features using a 20:1 reduction," Opt. Lett. 15(10), 529–531 (1990).
4. D. W. Berreman, J. E. Bjorkholm, M. Becker, L. Eichner, R. R. Freeman, T. E. Jewell, W. M. Mansfield, A. A. MacDowell, M. L. O'Malley, E. L. Raab, W. T. Silfvast, L. H. Szeto, D. M. Tennant, W. K. Waskiewicz, D. L. White, D. L. Windt, and O. R. Wood II, "Use of trilevel resists for high-resolution soft-x-ray projection lithography, Appl. Phys. Lett. 56(22), 2180–2182 (1990).
5. D. L. White, J. E. Bjorkholm, J. Bokor, L. Eichner, R. R. Freeman, J. A. Gregus, T. E. Jewell, W. M. Mansfield, A. A. MacDowell, E. L. Raab, W. T. Silfvast, L. H. Szeto, D. M. Tennant, W. K. Waskiewicz, D. L. Windt, and O. R. Wood, II, "Soft-x-ray projection lithography: experiments and practical printers," Proc. SPIE 1343, 204–213 (1990).
6. D. L. Shealy, R. B. Hoover, A. B. C. Walker, Jr., and T. W. Barbee, Jr., "Development of a normal incidence multilayer, imaging x-ray microscope," Proc. SPIE 1160, 109–121 (1989).
7. D. L. Shealy, D. R. Gabardi, R. B. Hoover, A. B. C. Walker, Jr., J. F. Lindblom, and T. W. Walker, Jr., "Design of a normal incidence multilayer imaging x-ray microscope," J. X-Ray Sci. Technol. 1, 190–206 (1989).
8. D. L. Shealy, R. B. Hoover, T. W. Barbee, Jr., and A. B. C. Walker, Jr., "Design and analysis of a Schwarzschild imaging multilayer x-ray microscope," Opt. Eng. 29(7), 721–727 (1990).
9. A. K. Head, "The two-mirror aplanat," Proc. Phys. Soc. LXX, 10-B, 945–949 (1957).
10. A. B. C. Walker Jr., J. F. Lindblom, R. H. O'Neil, M. J. Allen, T. W. Barbee Jr., and R. B. Hoover, "Multi-Spectral Solar Telescope Array," Opt. Eng. 29, 581–591 (1990).
11. P. C. Baker, "Advanced Flow-Polishing of exotic optical materials," Proc. SPIE 1160, 263–270 (1989).
12. W. P. Zmek, E. C. Moran, and J. E. Harvey, "Effects of surface quality upon the performance of normal incidence x-ray/XUV imaging systems," Proc. SPIE 984, 202 (1988).
13. J. E. Harvey, W. P. Zmek, and C. Ftaclas, "Image quality prediction of normal incidence x-ray/EUV multilayers in the presence of substrate and interface fabrication errors," Opt. Eng. 29, 603 (1990).
14. E. Spiller, R. McCorkle, J. Wilczynski, L. Golub, G. Nystrom, P. Takacz, and C. Welch, "Imaging performance and tests of soft x-ray telescopes," Proc. SPIE 1343, 134 (1990).
15. A. B. C. Walker, Jr., J. F. Lindblom, J. G. Timothy, R. B. Hoover, T. W. Barbee, Jr., P. C. Baker, and F. R. Powell, "High resolution imaging with multilayer FUV, EUV, and soft x-ray telescopes of modest aperture and cost," Proc. SPIE 1494-32, in press (1991).
16. R. B. Hoover, T. W. Barbee, Jr., P. C. Baker, J. F. Lindblom, M. J. Allen, C. DeForest, C. C. Kandelborg, and R. H. O'Neal, "Performance of compact multilayer coated telescopes at soft x-ray, EUV, and VUV wavelengths," Opt. Eng. 29, 1281 (1990).

17. R. B. Hoover, P. C. Baker, J. B. Hadaway, R. B. Johnson, D. R. Gabardi, A. B. C. Walker, Jr., J. F. Lindblom, C. E. DeForest, and R. H. O'Neal, "Performance of the multi-spectral solar telescope array III: optical characteristics of the Ritchey-Chrétien telescopes," Proc. SPIE 1343, 189 (1990).
18. R. C. Chase, "Aplanatic grazing incidence x-ray microscopes: design and performance," Appl. Opt. 15(12), 3094–3098 (1976).

David L. Shealy is a professor and the chair of the Department of Physics at the University of Alabama at Birmingham. He has designed a variety of x-ray telescopes and microscopes for NASA and is currently working with Los Alamos National Laboratory on the design of soft x-ray grazing incidence FEL cavities and application of soft x-ray FELs to projection lithography. Dr. Shealy has published a number of papers in x-ray and laser optics, caustic theory, and optics design, and is a fellow of the Optical Society of America.

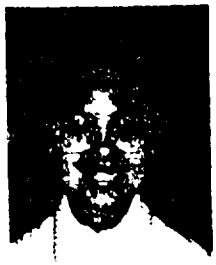

Wu Jiang is a Ph.D. student of the Department of Physics at the University of Alabama at Birmingham. She received the BS degree in optical engineering in 1983 from Zhejiang University in China and the MS degree in optics in 1986 from the Academy of Sciences of China. She is currently working on the design and analysis of multilayer x-ray microscopes.

Richard B. Hoover: Biography and photograph appear with the guest editorial in this issue.

APPENDIX 2

"Development of the water window imaging x-ray microscope utilizing normal-incidence multilayer optics"

Richard B. Hoover, David L. Shealy, B.R. Brinkley,

Phillip C. Baker, Troy W. Barbee, Jr., and Arthur B.C. Walker, Jr.

Optical Engineering, Vol. 30 No. 8, 1086-1093, (1991)

Development of the water window imaging x-ray microscope utilizing normal-incidence multilayer optics

Richard B. Hoover, MEMBER SPIE
NASA Marshall Space Flight Center
Space Science Laboratory
Huntsville, Alabama 35812

David L. Shealy, MEMBER SPIE
University of Alabama at Birmingham
Department of Physics
Birmingham, Alabama 35294

B. R. Brinkley
University of Alabama at Birmingham
Department of Cell Biology and Anatomy
Birmingham, Alabama 35294

Phillip C. Baker
Baker Consulting
Walnut Creek, California 94596

Troy W. Barbee, Jr., MEMBER SPIE
Lawrence Livermore National Laboratory
Livermore, California 94550

Arthur B. C. Walker, Jr., MEMBER SPIE
Stanford University
Center for Space Science and
Astrophysics
Stanford, California 94305

Abstract. We describe the development of the water window imaging x-ray microscope based on normal-incidence multilayer x-ray mirrors. The narrow bandpass response inherent in multilayer x-ray optics is accurately tuned to wavelengths within the "water window." Similar doubly-reflecting multilayer optical systems have been fabricated for our astronomical rocket-borne x-ray/EUV telescopes. Previous theoretical studies performed during the MSFC X-Ray Microscope Development Program established that high-resolution multilayer x-ray imaging microscopes are possible by using either spherical (Schwarzschild configuration) optics or aspherical configurations. These microscopes require ultrasmooth mirror substrates, which have been fabricated using advanced flow polishing methods. Hemlite-grade sapphire microscope optic substrates have been accurately figured and polished to a smoothness of 0.5-Å rms, as measured by the Zygo profilometer. We describe the current status of fabrication and testing of the optical and mechanical subsystems for the water window imaging x-ray microscope. This new instrument should yield images of carbon-based microstructures within living cells of unprecedented spatial resolution and contrast, without need for fixatives, dyes, and chemical additives.

Subject terms: x-ray EUV optics; water window imaging; multilayer x-ray optics; normal-incidence mirrors; Schwarzschild optics.

Optical Engineering 30(8), 1086-1093 (August 1991).

CONTENTS

1. BACKGROUND

In the past, considerable effort has been made to develop a microscope capable of operating within the "water window." This narrow x-ray spectrum regime lies between the K absorption edges of oxygen (23.3 Å) and of carbon (43.62 Å) and is of great value in the study of biological structures. The most important biological structures are dominantly carbon, but x-ray observations of these structures within living cells are greatly hindered due to the reduction in contrast that arises from x-ray absorption by the water contained within the cells. However, due to the nature of the interaction of x rays with matter, within this narrow band, carbon is highly absorptive, whereas water is relatively transparent. For this reason, this biologically important regime between 23.3 and 43.62 Å has been designated the *water window*. We anticipate that a high-resolution x-ray microscope operating exclusively within this regime should be capable of delineating, with unprecedented contrast, carbon-based structures within the aqueous physiological environments of living cells. Conventional x-ray microscopes, such as grazing-incidence Kirkpatrick-Baez or Wolter microscopes and Fresnel diffraction zone-plate systems, represent broadband imaging technologies. They transmit and focus x rays over a much broader bandpass than the specific wavelengths of the narrow water window. However, our successful solar observations[1] have shown that normal-incidence multilayer x-ray optics are capable of operating in a very precisely determined and accurately tunable portion of the x-ray spectrum. Indeed, the technology developed for astronomical observations of the sun is now being applied to the production of a high-resolution multilayer imaging x-ray microscope for operation within the water window. We briefly review these earlier results.

Invited paper XR-118 received Jan. 15, 1991; accepted for publication March 3, 1991. This paper is a revision of paper 1435-48 presented at the SPIE conference Techniques and Applications in Chemical and Materials Analysis, January 1991, Los Angeles, Calif. The paper presented there appears (unrefereed) in SPIE Proceedings Vol. 1435.

A Nike-boosted Black Brant sounding rocket was launched from the White Sands Missile Range, New Mexico, on October 23, 1987. The Stanford/MSFC/LLNL Rocket X-Ray Spectroheliograph on board produced the first high-resolution, narrow-wavelength-band x-ray/EUV images of the sun (Fig. 1) obtained with normal-incidence multilayer x-ray optics. Modern methods of fabricating stable normal-incidence multilayer optics are due to developments achieved only a decade ago by Barbee[2] and by Spiller.[3]

For the Stanford/MSFC/LLNL Rocket X-Ray Spectroheliograph program, Barbee fabricated 44-Å multilayer coatings on concave primary mirrors and concave secondary mirrors of a small Cassegrain x-ray telescope. Due to the precise bandpass matching required, two-element multilayer optical systems, such as used in these Cassegrains, are far more difficult to construct than are single-element (Herschelian) telescope systems. These doubly reflecting multilayer telescopes, which were operating in the water window at 44 Å, were tested at the MSFC X-Ray Calibration Facility and used to produce high-resolution, soft x-ray images of a laboratory source.[4] These laboratory and solar soft x-ray/EUV images constitute dramatic proof that normal-incidence multilayer coatings on curved surfaces can produce superb x-ray/EUV images. (We consider the wavelength regime 1 to 100 Å to be the soft-x-ray regime, and the 100 to 1000-Å range to constitute the extreme ultraviolet (EUV) regime.) During our rocket flight, high-density solar x-ray/EUV images were recorded on high-resolution photographic emulsions. The laboratory data with a doubly-reflecting Cassegrain operating at 44 Å and the solar images produced at 44 Å (with Wolter-Cassegrain optics), 173 Å (with Cassegrain optics), and 256 Å (with Herschelian and Cassegrain optics) have clearly demonstrated that multilayer coatings can yield excellent x-ray/EUV reflectivities and that the bandpasses of peak reflectivity of the two mirrors of a doubly-reflecting Cassegrain multilayer telescope or microscope system can be precisely matched.

Excellent reflectivity and precise bandpass matching have also been achieved for the primary and secondary optical elements of a new set of solar telescopes. This payload, known as the Multi-Spectral Solar Telescope Array (MSSTA),[5] is larger than its predecessor and was launched on a Terrier-boosted Black Brant sounding rocket on May 13, 1991. The 127-mm-aperture MSSTA telescopes, each with four times the collecting area of the Cassegrain telescope previously flown, employ Ritchey-Chrétien optical systems (Fig. 2). In these telescopes, the primary and secondary mirrors are hyperboloidal. These telescopes are "aplanatic," which means that the optical aberration known as coma is zero (to third order at least) and spherical aberration is absent. This design permits the telescopes to produce high spatial resolution images over a wide field of view. Theoretical calculations and laboratory studies of these instruments indicate that they should produce full-disk solar x-ray/EUV images with spatial resolution as high as 0.1 arc sec.[6]

The mirror substrates for the MSSTA telescopes were fabricated by Baker, using advanced flow polishing technology. Tests on the polished Zerodur mirror substrates revealed surfaces with 2-Å rms surface smoothness.[7] The mirror substrates were coated at LLNL using state-of-the-art multilayer coatings. Measurements at the NIST SURF II synchrotron and at the Stanford Synchrotron Radiation Laboratory have demonstrated that the multilayer coatings approach the performance expected for ideal multilayer structures.[8] The telescope mechanical structures were designed at Stanford, and fabricated, assembled, aligned, and tested interferometrically at MSFC. The success of the Stanford/MSFC/LLNL rocket x-ray spectroheliograph prompted us to initiate a program at MSFC to develop normal-incidence magnifying Schwarzschild x-ray microscope systems. The initial effort concentrated on the design, analysis, and development of normal-incidence multilayer x-ray microscope systems that could be used to couple x-ray telescopes to solid state detectors to increase the plate scale and enhance the system spatial resolution. Schwarzschild microscope systems were designed and analyzed, and the microscope mirror substrates were produced on Zerodur

Fig. 1. High-resolution 173-Å image of the sun produced with a doubly-reflecting Cassegrain multilayer x-ray telescope operating at normal incidence.

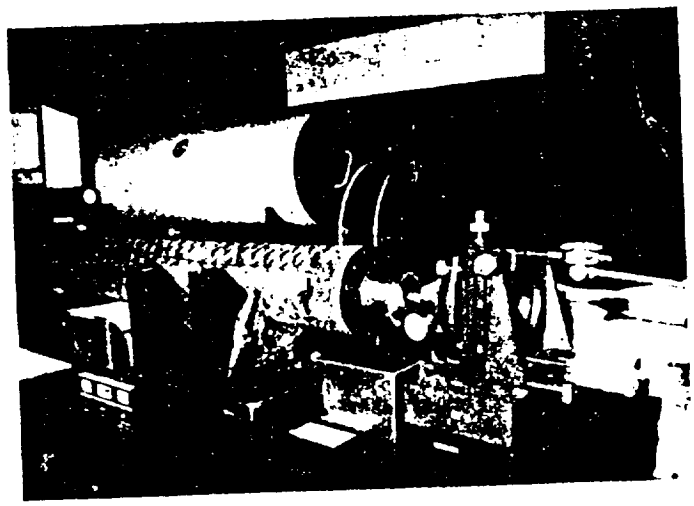

Fig. 2. Completed MSSTA Ritchey-Chrétien multilayer telescopes under interferometric test at MSFC. Telescope uses graphite epoxy tubes and mirror-mount technology similar to that planned for the water window imaging x-ray microscope.

blanks and advanced-flow-polished to a smoothness of 2 Å rms. Subsequently, contoured surfaces were fabricated for the microscopes with unprecedented rms smoothness from 0.5 to 0.6 Å on Hemlite-grade sapphire blanks by advanced flow polishing.

These profoundly important technological advancements in the ability to fabricate high-reflectivity, matched-bandpass, normal-incidence optics operating at 44 Å and the ability to produce the ultrasmooth substrates required by these coatings led us to conclude that a water window imaging x-ray microscope based on normal-incidence multilayer x-ray optical components is feasible. Such an instrument should yield entirely new optical methods for ultrasensitive detection of microstructure within living cells and affords great promise as a fundamental tool for basic cell biology and cancer research.

2. MULTILAYER X-RAY OPTICAL SYSTEMS

Multilayer x-ray mirrors are essentially synthetic Bragg crystals that can be deposited on flat mirrors or gratings or contoured to a figured surface. (For an overview of multilayer x-ray mirrors, see Barbee,[9] or refer to the numerous recent papers in volumes 1160 and 1343 of the SPIE Proceedings.[10,11]) Multilayer optics are fabricated by the accurate deposition on an ultrasmooth substrate of a coating consisting of a stack of many alternating layers of high-atomic-number (high-Z) diffractor material separated by layers of a low-Z spacer material. The layers must be uniform and of precisely repeatable thicknesses d_1 and d_2, respectively. Since this multilayer coating constitutes a synthetic Bragg crystal, x-ray reflection occurs by the process of Bragg diffraction. When slight refraction effects are ignored, the wavelength at which the peak of the reflectivity occurs is given by the Bragg relation $n\lambda = 2D \sin\theta$, where $D = d_1 + d_2$ and θ is the angle at which the radiation strikes the mirror, as measured from the mirror surface. For mirrors operating at normal incidence (θ = 90 deg), the equation becomes $\lambda = 2D$, where λ is the wavelength of peak reflectivity of the first-order Bragg diffracted light. Because D is the sum of the two layer thicknesses, a multilayer coating, designed to reflect 44-Å x rays, could be produced as a stack of alternating layers of a high-Z material (such as tungsten carbide) separated by layers of a low-Z spacer material (such as carbon), with each layer approximately 11 Å thick. Considering the dimensions involved, these layers are only a few atoms thick. Furthermore, the diffracting layers must be coplanar and uniform. The performance of a multilayer as an x-ray diffractor also critically depends on the nature of the interfaces between the low-Z and high-Z layers. Because the layers follow the contour of the substrate on which they are deposited, the smoothness and uniformity of multilayer optics substrates have stringent requirements. Especially this is important for layers with thicknesses in the 6- to 11-Å regime, which are required for systems designed to operate at normal incidence in the water window. For the multilayer coating to be an effective reflector, many diffractor and spacer layers must be in the stack and the thickness of each layer must be controlled to a very high degree of accuracy. Indeed, by choice of the D spacing and the materials constituting the multilayer coating, we can tailor the coating to reflect x-ray or EUV radiation within a selected very narrow bandpass.[12]

Although only a small fraction of the incident radiation is reflected at each low-Z/high-Z interface, by use of a stack of tens to hundreds of alternating layers in the coating, high reflectivities at normal incidence can be achieved by constructive interference if the layer pairs are deposited with sufficient uniformity. Recently, tests were performed at the Stanford Synchrotron Radiation Laboratory (SSRL) and the National Institute of Standards and Technology (NIST) SURF II synchrotron on the MSSTA telescopes.[8] These studies revealed that reflectivities approaching 45% at normal incidence were produced by the mirrors operating at 173 Å and 193 Å. For the MSSTA Ritchey-Chrétien and Herschelian telescopes in our solar rocket program, optics were fabricated with coatings on both convex and concave superpolished substrates whose reflectivities were peaked for soft x-ray and EUV radiation in the range 44 Å $< \lambda <$ 335 Å.

Since multilayer x-ray mirrors reflect x rays by Bragg diffraction, only a very narrow bandpass, wherein the Bragg condition is satisfied, is efficiently reflected. In the water window, multilayer mirrors can achieve spectral resolution ($\lambda/\Delta\lambda$) exceeding 50. This characteristic is of the utmost importance for the development of a water window imaging x-ray microscope. X rays of longer or shorter wavelength would seriously degrade the contrast of carbon structures within the cell, which is a major reason why grazing-incidence x-ray optics and Fresnel zone plates are not ideally suited for the fabrication of a water window x-ray imaging microscope. Zone-plate and grazing-incidence optics focus x rays over a much broader bandpass than the water window, which is required for high-contrast images. Furthermore, with zone plates, the radiation at different wavelengths will come to focus at slightly different points along the optical axis, further degrading the spatial resolution. Grazing-incidence optics are also highly sensitive to contaminants and x-ray scattering, and suffer far more severely from optical aberrations off-axis (offense against the Abbé sine condition, etc.) than do the normal-incidence multilayer x-ray optics. Because multilayer optics reflect in only a very narrow bandpass of the incident radiation, precise matching of the wavelength at which peak reflectivity occurs from the primary and secondary mirrors is required. If these bandpasses are not accurately matched, the net throughput of the instrument will be drastically reduced.

3. X-RAY IMAGING IN THE WATER WINDOW

The x-ray water window is biologically significant because water is prevalant in all living cells. The oxygen of the water plays the dominant role for the absorption of soft x rays. However, structures of the greatest scientific interest (such as organelles, cytoskeletal components, membranes, secretory vesicles, endoplasmic reticulum, chromatin, nucleoli, and nucleosomes) in general comprise complex molecules (DNA, RNA, proteins, etc.) incorporating large amounts of carbon. The nature of the interaction of x rays with matter makes it possible to observe these carbon structures with minimal interference from the surrounding water. A sharp discontinuity or "edge" in the absorption spectrum of a material occurs when the energy of the photon is sufficient to ionize electrons from one of the shells or subshells of the atoms of the material. These edges are designated by the shell or subshell from which the electrons are ejected, i.e., K for the innermost shell, L_I, L_{II}, and L_{III} for the sublevels of the next shell, etc. The strongest *absorption edges* are the K-edges. For wavelengths immediately below the K-edge, the absorptivity increases dramatically. Because x rays whose wavelength are longward of the K absorption edge do not have sufficient energy to eject a K-shell electron, they are not strongly absorbed by the material, which appears relatively transparent at these wavelengths.

For the purposes of x-ray microscopy, it is significant that the K absorption edge for the element oxygen lies at 23.3 Å,

and for carbon the K-edge is at 43.62 Å. This results in a narrow bandpass in the soft x-ray spectrum between 23.3 Å (oxygen K absorption edge) and 43.62 Å (carbon K absorption edge), called the water window. In this wavelength regime, water is relatively transparent and carbon is highly absorptive. The opacity of protein and water at these wavelengths has been calculated by London et al.[13] and is shown in Fig. 3. These results show the dramatic difference in the absorptivity of protein and water within the water window. The water window imaging x-ray microscope should make it possible to investigate carbon structures (and possibly even the motions of those structures) within the aqueous environment of living cells.

We have, therefore, initiated a program to fabricate an imaging x-ray microscope, utilizing ultrasmooth, advanced-flow-polished, and figured sapphire mirror substrates coated with multilayers, with 2D spacing such that 23.3 Å $< 2D <$ 43.62 Å, which is appropriate to reflect x rays of a narrow bandpass within the water window. At these wavelengths, ultrahigh-resolution photographic films (i.e., XUV 100 and XUV 649) and photoresists can be used as the x-ray detector. The Kodak 649 emulsion affords spatial resolution of 2000 lines/mm when processed for optimum resolution and has a very great dynamic range, and will serve as a primary detector for the instrument. However, resists are also utilized for some studies, because they can afford even higher spatial resolution than is achievable by the best photographic films.

The water window imaging x-ray microscope should be capable of producing high-resolution, high-contrast images of chromosomes, proteins, and other carbon structures within living or freshly killed cells. It should permit smaller structures to be resolved than is currently possible with visible light or fluorescence microscopy. By obtaining sequential images using high repetition rate, laser-plasma x-ray sources, it may be possible to investigate motions of genetic material, proteins, and other structures within living cells.

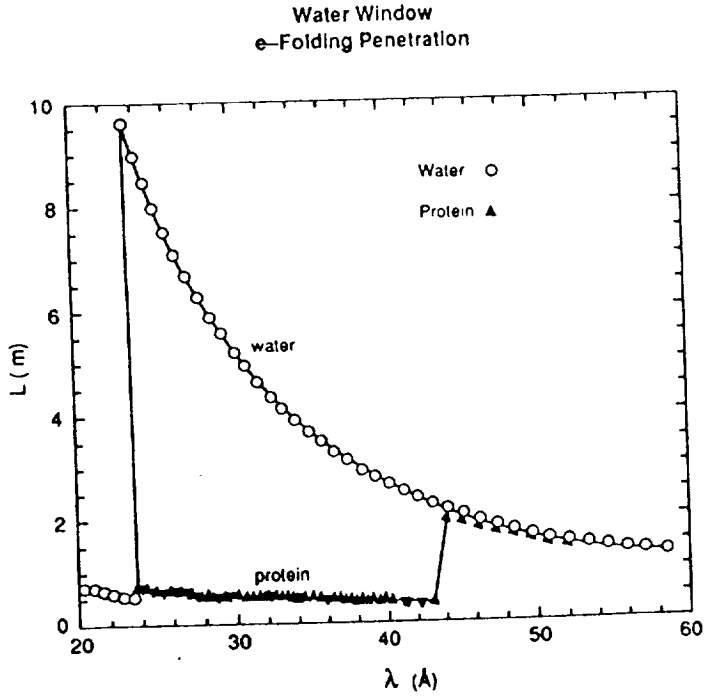

Fig. 3. E-folding penetration of x rays in the water window. (Redrawn after London et al.[13])

4. OPTICAL CONFIGURATION OF THE X-RAY MICROSCOPE

The optical ray trace codes and design methods that we utilized for the development of aplanatic normal-incidence multilayer x-ray telescopes have now been applied to the development of aplanatic imaging x-ray microscopes. In the initial investigations, we explored multilayer optical systems in the Schwarzschild configuration to produce imaging systems. Other workers have explored normal-incidence multilayer x-ray optics for use in scanning x-ray microscopes. Spiller[14] used elliptical multilayer mirrors for a scanning x-ray microscope. Trail and Byer[15] also fabricated a scanning microscope, and Lovas et al.[16] employed a Schwarzschild system for imaging applications in laser fusion research.

These efforts to utilize normal-incidence multilayer x-ray optics for the production of a high-resolution imaging x-ray microscope are relatively recent, and a considerable amount of work has occurred in the past in the use of Fresnel zone plates for x-ray microscopy. This approach was pioneered by Baez[17] in 1960. The technology of producing x-ray imaging Fresnel zone plates of extremely fine structure and high quality has advanced dramatically in the past few years by the use of holographic and electron-beam lithographic techniques, as described by Anderson.[18] Bionta et al.[19] have fabricated transmissive zone plates by sputtering a multilayer coating on 100-μm-diam wires, which are subsequently cut into thin slices. An excellent review of x-ray microscopes using zone-plate technology is given by Howells, Kirz, and Sayre.[20] Since Fresnel zone plates focus radiation by Fresnel diffraction, they do not afford the narrow-bandpass characteristics that are obtained with multilayer optics, which behave as synthetic Bragg crystals and reflect light by Bragg diffraction. The zone plate focuses radiation of different wavelengths to different positions along the optical axis, which can result in loss of resolution and contrast with polychromatic sources. This characteristic is particularly disadvantageous for the water window imaging x-ray microscope, wherein it is desired that only a narrow band of wavelengths within the water window be imaged to employ the selective absorption characteristics of carbon versus oxygen for contrast enhancement. Normal-incidence multilayer optics of the Schwarzschild configuration have the inherently narrow bandpass that is well suited for a high-resolution imaging x-ray microscope designed to operate in the water window.

Our prior studies of Schwarzschild multilayer microscopes were constrained to the development of systems for which high-smoothness spherical laser mirrors were available as off-the-shelf components. Suitable spherical substrates had been purchased from General Optics of Moorepark, CA, and were used for the telescopes flown on October 23, 1987. However, during the development of the MSSTA, Baker Consulting produced hyperboloidal optical substrates of Zerodur with ultrahigh smoothness (2 Å rms). Their fabrication methods can also yield spherical or aspherical substrates that are ideal for x-ray microscopes. High-resolution aplanatic imaging x-ray microscopes configured from low-x-ray scatter, normal-incidence multilayer optics should find important applications in many areas, including laser fusion research, x-ray lithography, materials science, astronomy, genetic engineering, virology, and bacteriology, as well as fundamental cell biology and cancer research.

We designed and analyzed several Schwarzschild x-ray microscope configurations. Diffraction analysis indicates that better than 200-Å spatial resolution in the object plane for up to a

1-mm field of view can be achieved with 125-Å radiation. Since the diffraction limit scales with the wavelength, when the microscope is used with 37-Å radiation (within the water window) spatial resolution below 100 Å may be realized. We are currently fabricating 20× and 30× normal-incidence multilayer x-ray microscopes of 1.35 m overall length. An aplanatic x-ray microscope using two spherical mirrors can be constructed by imposing the Schwarzschild condition on the selection of the mirror radii. The Schwarzschild condition can best be understood by referring to Fig. 4.

The mirror surfaces S_1 and S_2 are concentric spherical surfaces of radii R_1 and R_2, respectively. A complete discussion of the ray trace analysis of a Schwarzschild microscope configured for normal-incidence multilayer applications was presented by Hoover et al.[21] and Shealy et al.[22] The Schwarzschild condition for an aplanatic, two-mirror imaging system can be expressed:

$$\frac{R_2}{R_1} = 1.5 - \frac{R_2}{Z_0} \pm \left[1.25 - \frac{R_2}{Z_0}\right]^{1/2}, \qquad (1)$$

where the + sign is used in Eq. (1) for magnifications greater than 5 and the − sign is used for magnifications less than 5. Hoover et al.[21] have summarized the Schwarzschild design equations and presented the dependence of the rms blur circle radius as a function of the object height, image plane location, mirror tilts, and decentration for a 10× microscope with a total length of 1.41 m. As the magnification increases, so does the overall length of the microscope. The parameters for systems varying in magnifications from 2× to 50× have been computed and are given in Table 1.

We have calculated the spatial resolution, transmission losses due to vignetting, and off-axis performance for the 20× and 30× Schwarzschild x-ray microscopes, which we are currently fabricating. These calculations imply that to take advantage of their inherently high spatial resolution, we need photographic emulsions capable of achieving 0.78-μm spatial resolution. This implies the need for films capable of resolving better than 1300 lines/mm over a 20-mm-diam regime. We have established that the Kodak 649 emulsion has the required spatial resolution and is sensitive over the soft x-ray/EUV portions of the spectrum.[23]

TABLE 1. Schwarzschild x-ray microscope system parameters.

M(x)	R_1 (cm)	R_2 (cm)	s (cm)	d (cm)	Z (cm)	f (cm)
2	108.00	10.00	18.25	98.00	−91.42	5.51
3	58.27	10.00	18.05	48.27	−34.12	6.04
4	45.58	10.00	18.01	35.58	−13.56	6.41
5	40.00	10.00	18.00	30.00	0.0	6.67
10	31.79	10.00	18.02	21.79	48.36	7.29
15	29.69	10.00	18.04	19.69	91.04	7.54
20	28.75	10.00	18.05	18.75	131.49	7.67
30	27.84	10.00	18.06	17.84	213.27	7.80
40	27.40	10.00	18.07	17.40	296.07	7.87
50	27.15	10.00	18.07	17.15	376.42	7.92

Even higher spatial resolution may be achieved through aspherical optics. We have carried out a theoretical design and analysis of aspheric x-ray microscope configurations, which yield far better resolution over a wider field of view than is possible with the Schwarzschild configuration.[24] Results of the analysis of the aspherical 20× microscope also reveal that superior off-axis performance due to reductions in coma can be achieved.

5. FABRICATION OF THE X-RAY MICROSCOPE

The 20× and 30× Schwarzschild x-ray microscopes now being fabricated utilize much of the technology implemented in the MSSTA program. The microscope systems will initially be utilized in conjunction with synchrotrons and laser fusion sources, so great care and attention was paid to the selection of materials that are compatible with the ultrahigh vacuum requirements of beam lines. In addition, a conical mechanical structure was selected, to conform to the beam clearance requirements of the OMEGA laser fusion facility of the Laboratory for Laser Energetics of the University of Rochester.

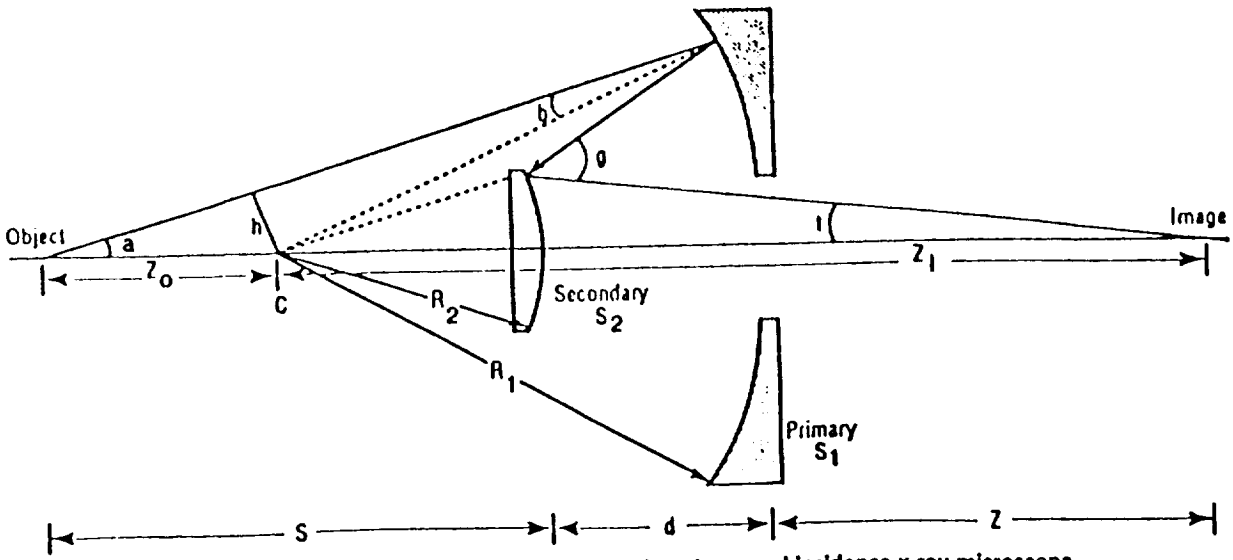

Fig. 4. Schwarzschild configuration for an aplanatic normal incidence x-ray microscope.

5.1. Optical components

The x-ray microscope mirror substrates were fabricated by Baker Consulting, using Zerodur and Hemlite-grade sapphire materials. It is very important that the mirror substrate material have the ability to be polished to an ultrasmooth finish but have low thermal expansion coefficient. Although sapphire has somewhat higher thermal expansion properties than Zerodur, it can be polished to phenomenal smoothness. In addition, the subsurface condition of the mirror substrate must be considered as a possible factor in the performance, due to possible stress relaxation during coating or from externally applied force, either thermal or mechanical. During fabrication of sapphire surfaces, it has been demonstrated that the use of the advanced flow polishing technique has produced a zero subsurface damage condition as measured with Rutherford backscatter techniques by General Ionex Corp.

The primary mirrors were fabricated as concave spheres of 8 cm outside diameter. They have a radius of curvature of 23 cm and a central hole diameter of 2.2 cm. The convex spherical secondaries have 2-cm diameter with an 8-cm radius of curvature. The sapphire optical surfaces were polished to 0.5- to 0.6-Å rms surface smoothness, and had surface figure accuracy better than $\lambda/10$ when tested with visible light. The mirror substrate smoothness was measured with a Zygo profilometer, and the completed optical systems were tested by interferometric techniques at visible wavelengths to ensure that the precise optical figure of the elements was obtained. Final performance testing of the completed x-ray microscope assembly will be carried out by producing images of microscopic structures with the instrument at x-ray wavelengths. These tests require the use of ultrahigh resolution photographic emulsions and high-intensity x-ray sources. Initial studies will be carried out using the laser fusion plasma produced by the OMEGA facility of the University of Rochester and with x-ray/EUV emission generated by the NIST SURF II or the SSRL synchrotron facilities. All microscope structures have been designed and are currently being fabricated. The mount structures have a conical configuration so as to be compatible with the beam constraints of the OMEGA facility. The x-ray microscope currently being fabricated is shown in Fig. 5.

5.2. Mechanical components

The microscope tube structures were fabricated by filament winding methods that used AS4-12K graphite fiber with an HBRF55A epoxy resin matrix. Longitudinal fibers were applied to increase stiffness and to produce microscope tube structures with near-zero coefficient of thermal expansion. This technique is the same as that used to fabricate the tube structures for the 127-mm-diam telescopes for MSSTA. The primary and secondary mount cells were fabricated utilizing the same approach that we have employed for the MSSTA telescope optics. The mirrors will be mounted in their respective cells by means of a low-outgassing silicone rubber. The mount tube structures are constructed of nonmagnetic stainless steel.

5.3. Filters, cameras, and film

Filters will be used to ensure that only x-ray emissions transmitted by the specimen and imaged by the microscope reach the image plane. Filtering will be accomplished by thin foil metal filters as specimen holders and as prefilters placed in front of the camera film plane. This double-filter approach results in a reduction of the light levels reaching the film, but with the high-intensity sources we plan to utilize for the tests no problems should occur. Thin-film filters of 1500-Å aluminum on a nickel support mesh and of phthalocyanine/carbon have been fabricated by the Luxel Corp. of Friday Harbor, Washington. These filters will be used as specimen supports and visible-light rejection filters. The microscope camera adapters accommodate either the 35-mm Canon T-70's, which were flown on the rocket x-ray spectroheliograph, or the 70-mm Pentax 645 MSSTA cameras. Primary data recording will be on photographic film, utilizing experimental XUV-100, 101-07, and XUV 649 emulsions. We have studied these photographic emulsions at selected wavelengths in the soft x-ray/EUV/FUV, ranging from 44 to 1550 Å. X-ray exposures have been obtained to evaluate resolution and response characteristics in tests carried out at the MSFC X-Ray Telescope Test Facility, the Los Alamos National Laboratory, the Stanford Synchrotron Radiation Laboratory and the SURF II synchrotron of the National Institute of Standards and Technology.[23-25] Other groups have concentrated on the use of photoresists, which have higher spatial resolution than photographic emulsions. We also plan to utilize photoresists for the highest resolution investigations. However, our initial work will be carried out using high-resolution photographic emulsions, which are typically from 100 to 1000 times more sensitive than photoresists. Consequently, images will be obtainable with significantly shorter exposure times.

6. MEASURED PERFORMANCE OF X-RAY MICROSCOPE OPTICS

The completed x-ray microscope optical systems have been tested interferometrically and found to have rms wavefront errors less

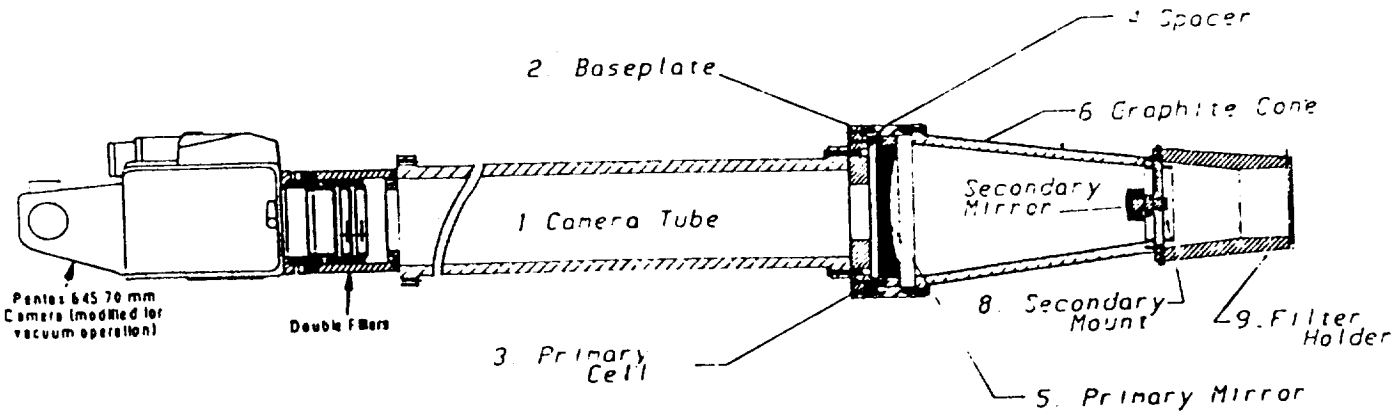

Fig. 5. Structural configuration of the water window imaging x-ray microscope.

than λ/100. Figure 6 shows the measured geometric radial energy distribution of the 20× Zerodur Schwarzschild mirror system. It can be seen that 90% of the energy is contained within 0.12 Airy disk radii. The point spread function of this system, as determined by interferometric analysis of the optics, is shown in Fig. 7.

The first Schwarzschild microscope prototype x-ray optics are being coated with multilayers for operation at 130 to 135 Å. Normal-incidence reflectivities better than 55% have been experimentally achieved from multilayers on concave surfaces in this wavelength range. Based upon the theoretical analysis and measurements of the optical characteristics of the completed mirrors that we have performed, we anticipate that a spatial resolution of 300 to 400 Å in the object plane should be obtainable with a Schwarzschild microscope operating at an initial test wavelength of 130 to 135 Å. In the water window with mirrors of the same design coated to reflect radiation of 36 to 40 Å wavelength, significantly better spatial resolution should be realized. After final assembly and optical alignment of the multilayer microscope at MSFC, x-ray tests and utilization of the instrument for imaging applications will begin at SSRL, SURF II, and the OMEGA facility. The imaging and assessment

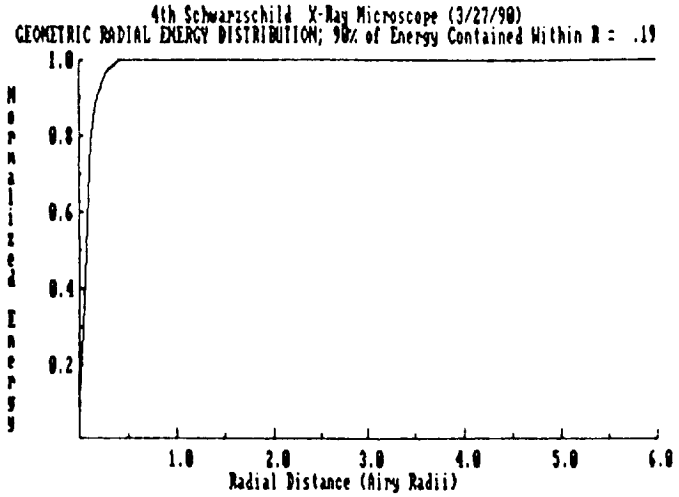

Fig. 6. Multipass interferometer measurements of the geometric radial energy distribution for the 20× Schwarzschild sapphire x-ray microscope optics.

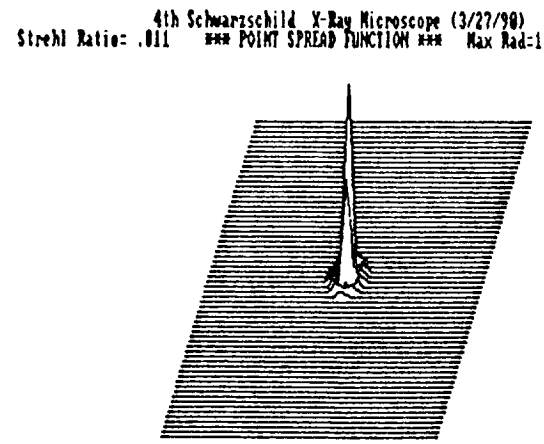

Fig. 7. Multipass interferometric determination of the point spread function for the 20× Schwarzschild sapphire microscope optical system.

phase at synchrotrons and the laser fusion facility could be accomplished within a year.

The requirements for the performance of the optical systems have become more exacting, driven by the high quality of the multilayer coatings and the demands of the imaging requirements at the shorter wavelengths. This has led to our use of special optical testing techniques for the measurement of the surfaces and the contours of the microscope and telescope optics. The standard interferometric analysis at the longer wavelengths (i.e., 6328-Å helium-neon line) has limitations, especially when the wavelength of use is considerably shorter, such as in water window microscope systems. The use of higher-sensitivity interferometric testing techniques, or the construction of an x-ray interferometer utilizing multilayer optics, is becoming essential due to the direct effect that system wavefront errors have on imaging quality. Existing techniques, such as multipass interferometry and holographic interferometry, have been used to increase the sensitivity of wavefront error detection.

These techniques must be improved as the wavelength shortens, especially in the area of aspherical system testing. Current designs that have been used involve spheres, but we are considering systems employing aspherical mirrors with both moderate and severe aspherical departures, with unusual contours that are not easily tested. Multipass interferometry was used with great success on the MSSTA Ritchey-Chrétien telescope systems in ensuring the accuracy of the systems. Employing these tests during the manufacturing of the individual components as well as the final system is extremely important. The use of multipass interferometry was made easier due to the highly reflective surface of the multilayers even at the longer test wavelength. The analysis was thus more exact, and the assessment of the performance at the shorter wavelengths has become more reliable.

7. APPLICATIONS TO TUMOR RESEARCH

Our current knowledge of tumor cell biology, detection, and diagnosis has been made possible by steady improvements in microscopic methods for examining cells and tissues. Knowledge of cell ultrastructure made possible by high-resolution transmission electron microscopy has revolutionized our concept of the organization of eukaryotic cells and the identification of organelles in the nucleus and cytoplasm. Recently, improvements in visible-light instrumentation have led to the development of enhanced methods for the study of tumor cell growth and malignancy and premalignant changes. For example, fluorescence microscopy, phase microscopy, differential interference contrast, and polarizing microscopy have provided new approaches for research into premalignant changes and improvements in diagnosis. Moreover, the availability of low-light-level video cameras and computer enhancements of digitized images have led to improved resolution of the structures in motile cells. All current optical techniques are limited due to relatively low resolution and low contrast of biological materials and the need, in most cases, for harsh fixatives, dyes, and chemical additives.

The water window imaging x-ray microscope has several potential features that could revolutionize tumor cell biology and cancer diagnosis. Its unique potential for detecting structures with spatial resolution in the object plane of 100 Å or better, along with its capacity to image living cells in aqueous, physiological environments, is an advantage that is not available in any conventional microscopes. Although initial trials would be limited to cell monolayers in tissue culture, imaging could be

extended to living tumor cells as well as analysis of frozen sections. Working with tumor cell biology specialists, we will mount cell samples for study. Images will be obtained at x-ray wavelengths in the water window portion of the spectrum using high-intensity synchrotron radiation sources. Computer analysis of the images will be carried out. These detailed laboratory/clinical tests and evaluation studies will provide the necessary data to establish the applicability of the water window imaging x-ray microscope to tumor research.

8. CONCLUSIONS

We have demonstrated theoretically that the Schwarzschild configuration affords a feasible approach for an imaging x-ray microscope. The development of advanced flow polishing methods permits the ultrasmooth substrates that are demanded by the state-of-the-art multilayer coatings that must be produced to yield an x-ray microscope capable of operating within the biologically important water window regime between 23.3 and 43.7 Å. We have successfully fabricated the necessary mirror substrates and mechanical structures and anticipate that the initial tests of the prototype microscope will be completed later this year.

The successful completion of this project could result in the production of an entirely new optical imaging method for ultrasensitive detection that should permit the study of living tumor cells with unprecedented spatial resolution. It may allow the structures within the cells to be studied without the introduction of fluorescent dyes or chemical additives, which can alter the cellular processes under study. If the full optical potential is realized, the water window imaging x-ray microscope could become a standard diagnostic instrument in hospitals and medical centers throughout the world. It is envisioned that commercial instruments could be integrated with compact, internally contained, high-intensity laser-plasma x-ray sources. Its potential as an essential microscope for fundamental cell research would ensure its commercial application in research centers and universities.

9. ACKNOWLEDGMENTS

We wish to express gratitude to Jim Williams, Dale Wassermann, Dennis McCann, and Bob Carter at MSFC for their efforts in the fabrication of the critical mechanical components of the microscope and to Forbes R. Powell of LUXEL Corp. for the fabrication of the x-ray filters and specimen mounts. We also wish to acknowledge that this work is supported by MSFC Center Director's Discretionary Fund and NASA grant NSG-5131, and by the U.S. Department of Energy through Lawrence Livermore National Laboratory under contract no. W-7405-Eng-48.

10. REFERENCES

1. A. B. C. Walker, Jr., T. W. Barbee, Jr., R. B. Hoover, and J. F. Lindblom, "Soft x-ray images of the solar corona with a normal incidence Cassegrain multilayer telescope," *Science* 241, 1781 (1988).
2. T. W. Barbee, Jr., "Sputtered layered synthetic microstructure [LSM] dispersion elements," AIP Proc. 75, 131 (1981).
3. E. Spiller, "Evaporated multilayer dispersion elements for soft x-rays," AIP Proc. 75, 124 (1981).
4. J. F. Lindblom, A. B. C. Walker, Jr., R. B. Hoover, T. W. Barbee, Jr., R. A. VanPatten, and J. G. Gill, "Soft x-ray/extreme ultraviolet images of the solar atmosphere with normal incidence multilayer optics," Proc. SPIE 982, 316 (1988).
5. A. B. C. Walker, Jr., J. F. Lindblom, R. H. O'Neal, M. J. Allen, T. W. Barbee, Jr., and R. B. Hoover, "Multi-spectral solar telescope array," *Opt. Eng.* 29, 581 (1990).
6. R. B. Hoover, P. C. Baker, J. B. Hadaway, R. B. Johnson, C. Peterson, D. R. Gabardi, A. B. C. Walker, Jr., J. F. Lindblom, and C. DeForest, "Performance of the Multi-Spectral Solar Telescope Array, III: optical characteristics of the Ritchey-Chrétien and Cassegrain telescopes," in *X-ray/EUV Optics for Astronomy, Microscopy, and Projection Lithography*, R. B. Hoover and A. B. C. Walker, Jr., eds., Proc. SPIE 1343, 187 (1990).
7. P. C. Baker, "Advanced flow-polishing of exotic optical materials," in *X-ray/EUV Optics for Astronomy and Microscopy*, R. B. Hoover, ed., Proc. SPIE 1160, 263 (1989).
8. T. W. Barbee, Jr., J. W. Weed, R. B. Hoover, M. J. Allen, J. F. Lindblom, R. H. O'Neal, C. C. Kankelborg, C. E. DeForest, E. S. Paris, A. B. C. Walker, Jr., T. D. Willis, E. Gluskin, P. Pianetta, and P. C. Baker, "The Multi-Spectral Solar Telescope Array II: soft x-ray/EUV reflectivity of the multilayer mirrors," *Opt. Eng.* 30(8), 1067–1075 (1991).
9. T. W. Barbee, Jr., "Multilayers for x-ray optics," *Opt. Eng.* 25, 898 (1986).
10. R. B. Hoover, ed., *X-ray EUV Optics for Astronomy and Microscopy*, Proc. SPIE 1160 (1989).
11. R. B. Hoover and A. B. C. Walker, Jr., eds., *X-ray/EUV Optics for Astronomy, Microscopy and Projection Lithography*, Proc. SPIE 1343 (1990).
12. A. E. Rosenbluth, "Computer search for layer materials that maximize the reflectivity of x-ray multilayers," *Rev. Phys. Appl.* 23, 1599 (1988).
13. R. A. London, M. D. Rosen, and J. E. Trebes, "Wavelength choice for soft x-ray laser holography of biological samples," *Appl. Opt.* 28, 3397 (1989).
14. E. Spiller, "A scanning soft x-ray microscope using normal incidence mirrors," in *X-ray Microscopy*, G. Schmahl and D. Rudolph, eds., pp. 226–221, Springer-Verlag, Berlin (1984).
15. J. A. Trail and R. L. Byer, "X-ray microscope using multilayer optics with a laser induced plasma source," Proc. SPIE 563, 90 (1985).
16. I. Lovas, W. Santy, E. Spiller, R. Tibbits, and J. Wilczynzki, "Design and assembly of a high resolution Schwarzschild x-ray microscope for soft x-rays," Proc. SPIE 316, 90 (1982).
17. A. V. Baez, "A self-supporting Fresnel zone-plate to focus extreme ultraviolet and soft x-rays," *Nature* 186, 958 (1960).
18. E. Anderson, "Fabrication technology and applications of zone plates," in *X-ray/EUV Optics for Astronomy and Microscopy*, R. B. Hoover, ed., Proc. SPIE 1160, 2 (1989).
19. R. M. Bionta, E. Ables, O. Clamp, O. D. Edwards, P. C. Gabriele, D. Makowiecki, L. L. Ott, K. M. Skulina, and N. Thomas, "8 keV x-ray zone plates," in *X-ray EUV Optics for Astronomy and Microscopy*, R. B. Hoover, ed., Proc. SPIE 1160, 12 (1989).
20. M. R. Howells, J. Kirz, and David Sayre, "X-ray microscopes," *Scientific American* 264(2), 88 (1991).
21. R. B. Hoover, D. L. Shealy, D. R. Gabardi, A. B. C. Walker, Jr., J. F. Lindblom, and T. W. Barbee, Jr., "Design of an imaging microscope for soft x-ray applications," Proc. SPIE 984, 234 (1988).
22. D. L. Shealy, D. R. Gabardi, R. B. Hoover, A. B. C. Walker, Jr., J. F. Lindblom, and T. W. Barbee, Jr., "Design of a normal incidence multilayer imaging x-ray microscope," *J. X-ray Sci. Technol.* 1, 190 (1989).
23. R. B. Hoover, C. DeForest, J. F. Lindblom, R. H. O'Neal, C. Peterson, and A. B. C. Walker, Jr., "Performance of the Multi-Spectral Solar Telescope Array VI: performance of photographic film," in *X-ray/EUV Optics for Astronomy, Microscopy and Projection Lithography*, R. B. Hoover and A. B. C. Walker, Jr., eds., Proc. SPIE 1343, 175 (1990).
24. D. L. Shealy, W. Jiang, and R. B. Hoover, "Design and analysis of aspherical multilayer imaging x-ray microscope," in *X-ray/EUV Optics for Astronomy, Microscopy and Projection Lithography*, R. B. Hoover and A. B. C. Walker, Jr., eds., Proc. SPIE 1343, 122 (1990).
25. R. B. Hoover, T. W. Barbee, Jr., J. F. Lindblom, and A. B. C. Walker, Jr., "Solar soft x-ray XUV imagery with an experimental Kodak T-max film," *Kodak Tech Bits*, 1-6 (1988).

Richard B. Hoover: Biography and photograph appear with the guest editorial in this issue.

David L. Shealy: Biography and photograph appear with the paper "Design and analysis of aspherical multilayer imaging x-ray microscope" in this issue.

Troy W. Barbee: Biography and photograph appear with the paper "Multi-Spectral Solar Telescope Array II: soft x-ray EUV reflectivity of the multilayer mirrors" in this issue.

Arthur B.C. Walker, Jr.: Biography appears with the paper "Multi-Spectral Solar Telescope Array II: soft x-ray/EUV reflectivity of the multilayer mirrors" in this issue.

Biographies and photographs of other authors not available.

APPENDIX 3

"Design and analysis of soft x-ray imaging microscopes"

David L. Shealy, Cheng Wang,

Wu Jiang and Richard B. Hoover

Preprint of publication to appear in Proc. SPIE **1546** (1991)

SPIE International Symposium on Optical Applied Science and Engineering, July 21-26, 1991, San Diego, Proceedings SPIE 1546-22.

Design and analysis of soft x–ray imaging microscopes

David L. Shealy, Cheng Wang, Wu Jiang

Department of Physics
University of Alabama at Birmingham
Birmingham, AL 35295
205–934–8068

Richard B. Hoover

Space Science Laboratory
NASA/Marshall Space Flight Center
Huntsville, AL 35812
205–544–7617

ABSTRACT

Considerable efforts have been devoted recently to the design, analysis, fabrication, and testing of spherical Schwarzschild microscopes for soft x–ray applications in microscopy and projection lithography. The spherical Schwarzschild microscope consists of two concentric spherical mirrors configured such that the third order spherical aberration and coma are zero. Since multilayers are used on the mirror substrates for x–ray applications, it is desirable to have only two reflecting surfaces in a microscope. In order to reduce microscope aberrations and increase the field of view, generalized mirror surface profiles have been considered in this study. Based on incoherent and sine wave modulation transfer function (MTF) calculations, the object plane resolution of a microscope has been analyzed as a function of the object height and numerical aperture (NA) of the primary for several spherical Schwarzschild, conic, and aspherical Head reflecting two–mirror microscope configurations. The Head microscope with a NA of 0.4 achieves diffraction limited performance for objects with a diameter of 40 microns. Thus, it seems possible to record images with a feature size less than 100 Å with a 40x microscope when using 40 Å radiation.

1. INTRODUCTION

Recent experiments[1-3] in projection lithography have demonstrated that the Schwarzschild configuration of a reflecting microscope (see Fig. 1) will produce high resolution soft x–ray images. These experiments have used spherical mirror substrates coated with appropriate multilayers such that 500 Å features have been recorded on photoresist[2] using 130 Å radiation. Several design studies[4-6] have predicted that a spherical Schwarzschild configuration would be able to produce images with this level of spatial resolution. Since the spherical Schwarzschild microscope has only been corrected for third order spherical aberration and coma, these microscopes achieve their best resolution[7] when used with a small numerical aperture (NA) in the range of 0.1 to 0.14. For larger NA, the aberrations of the spherical Schwarzschild microscope degrade image resolution significantly.

In Ref. 7, the authors considered the advantages of using an aspherical two–mirror microscope. It was shown that diffraction limited resolution could be achieved for a NA of 0.22 when conic mirrors are used in a soft x–ray microscope. It was also noted in Ref. 7 that A. K. Head[8] presented an analytical solution for the differential equations of an aspherical two–mirror microscope in a general configuration where both the Abbe Sine Condition and the Constant Optical Path Length Condition are rigorously satisfied for all rays. Efforts were made to analyze the optical performance of a Head microscope by fitting the Head mirror surface profiles with a

conventional optics surface equation in the form

$$z(h) = \frac{c\ h^2}{1 + [1 - (\kappa + 1)\ c^2\ h^2]^{\frac{1}{2}}} + dh^4 + eh^6 + fh^8 \qquad (1)$$

where c is the curvature, h is the height of a ray from the optical axis, κ is the conic constant, and (d, e, f) are the aspherical coefficients. However, it was reported in Ref. 7 that a general aspherical microscope described by the surface equation (1) could only achieve performance similar to that of a conic system, which means that Eq. (1) does not adequately represent the surfaces of a Head microscope. One of the design equations of the Head microscope is the Constant Optical Path Length Condition, which means that for an on–axis point source the Head microscope should produce a spherical wave incident upon the image plane for all NA. Thus, the Head microscope should achieve diffraction limited performance for on–axis objects.

In order to overcome the inability of Eq. (1) to accurately describe the optical performance of the Head microscope, multiple sets of cubic spline functions have been used to fit the sag and slope of each Head microscope mirror. Then, a ray tracing program was developed for systems described in terms of multiple cubic spline functions. The optical performance of these systems has been analyzed by using the GENII OTF program.[9] Results of this study show that the optical performance of a Head microscope is near diffraction limited for large NA's and is significantly better than conics.

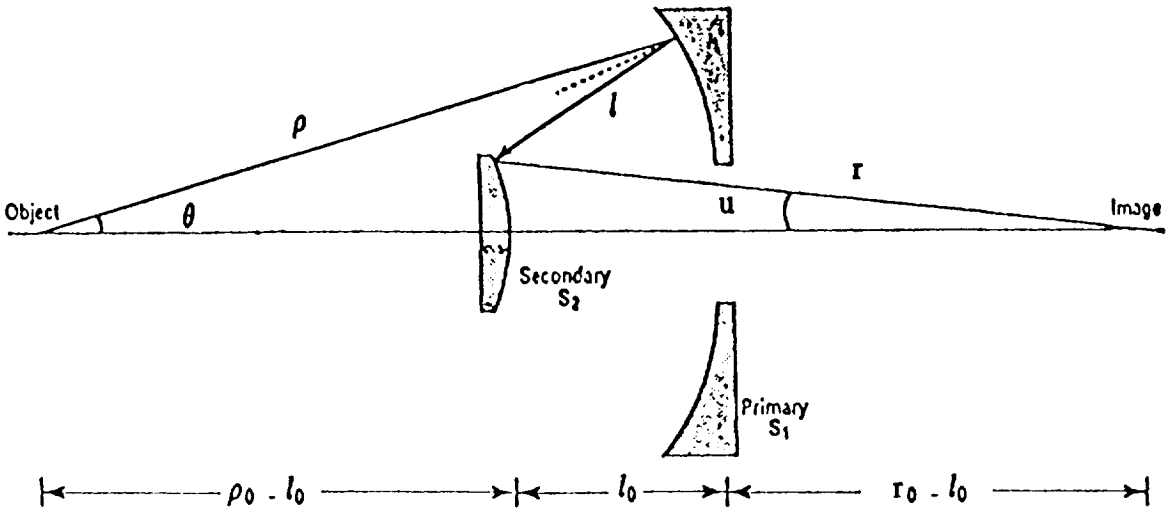

Fig. 1. Generalized two–mirror microscope configuration.

2. RESULTS

The spherical Schwarzschild microscope mirror parameters are given in Table 1 of Ref. 6 for magnifications varying from 2x to 50x. These Schwarzschild microscope parameters are based on the assumption that the radius of curvature of the secondary mirror is 10 cm. The Head microscope surface shapes can be evaluated from Eqs. (3–4) in Ref. 7. Previously, a 20x reflecting microscope has been studied[6-7] for operation with 100 Å radiation. The secondary mirror in this 20x microscope has a radius of curvature of 8 cm. Fabrication of this 20x spherical Schwarzschild

microscope is in progress, and experimental results are expected this year for operation with 130 Å radiation.

In this paper, modeling results of the optical performance of spherical, conic, and Head 40x reflecting microscopes with a secondary radius of curvature of 5 cm will be presented. The 40x systems have been configured to operate within the water window at 40 Å.[10] For a practical soft x–ray microscope, it is planned to use film as the detector which has a capability to record features with a spatial resolution in the image plane of 2,000 lp/mm. It is also possible to use photoresist as a detector in the image plane with a capability of resolving image features as small as 100 Å. However, photoresist requires a high contrast corresponding to a MTF of 40–50% to record an image. To obtain a measure of the object plane resolution, one typically divides the image plane resolution (defined in terms of the system achieving a specified MTF) by the system magnification. For microscope applications, it is convenient to use the object space numerical aperture, NA (=sinθ), instead of the image space numerical aperture, NA_{im} (=sinu). However, from the Abbe Sine Condition

$$NA = M\, NA_{im}. \tag{2}$$

Equation (2) can be used to convert the numerical aperture from object to image space. In the following results, the object space NA is used as the independent variable.

Figure 2 presents the object resolution versus the NA for spherical, conic, and the Head microscopes for an on–axis object point. As previously noted for on–axis objects,[7] the spherical Schwarzschild microscope achieves diffraction limited performance for NA $\leq$ 0.15, and the conic microscope is diffraction limited for NA $\leq$ 0.22. However, the Head microscope is diffraction limited for all NA when the object point is on–axis.

Using the diffraction limited resolution formula, which is based on the Rayleigh criterion for resolution,

$$Res = \frac{\lambda}{2NA}, \tag{3}$$

one can calculate the diffraction limited resolution of a spherical microscope to be 133 Å and of a conic microscope to be 91 Å when 40 Å radiation is used. For a Head microscope, a diffraction limited resolution of 67 Å with NA = 0.3 and 50 Å with NA = 0.4 can be achieved when using 40 Å radiation. It is interesting to note that Fig. 2 is consistent with these diffraction limited calculations.

Figure 3 presents the object resolution versus NA for the 40x Head microscope using 40 Å radiation when the source is displaced from the optical axis by the distance OH = 10, 20, 35, and 50 microns. These results show that a Head microscope will yield diffraction limited performance for objects with a diameter of 40 microns and a NA almost equal to 0.4. It is interesting to contrast the off–axis performance of a Head microscope to that of a conic microscope shown in Fig. 4. A conic microscope will yield near diffraction limited performance for objects with a diameter of 100 microns for a NA = 0.22. Figure 5 displays a plot of the deviation of the Head microscope surfaces from the best fit spherical surface versus the aperture radius. The NA varies from 0.08 for an aperture radius of 1–5 cm to 0.40 for an aperture radius of 7.5 cm. It is important to note that the aspherical surfaces of a Head microscope differs by less than 2 microns for all systems considered. Thus, only moderate aspherical surfaces are required to make a 40x Head microscope.

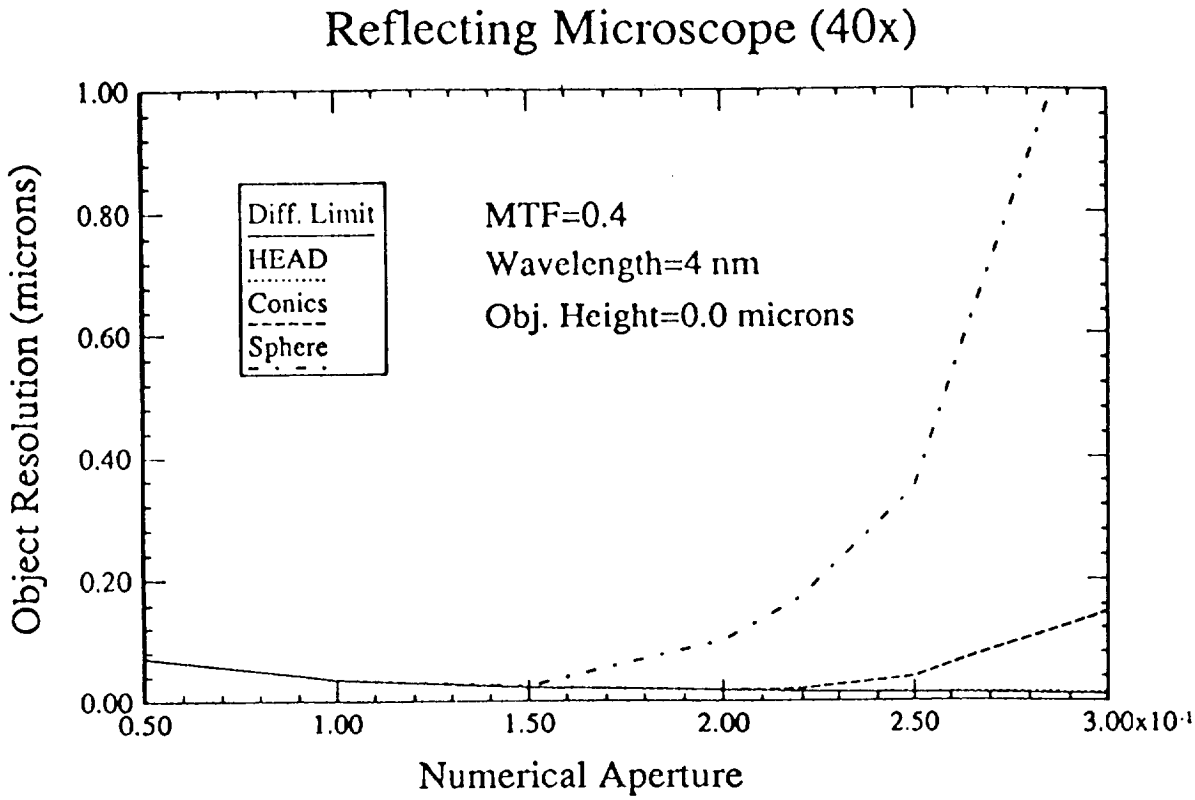

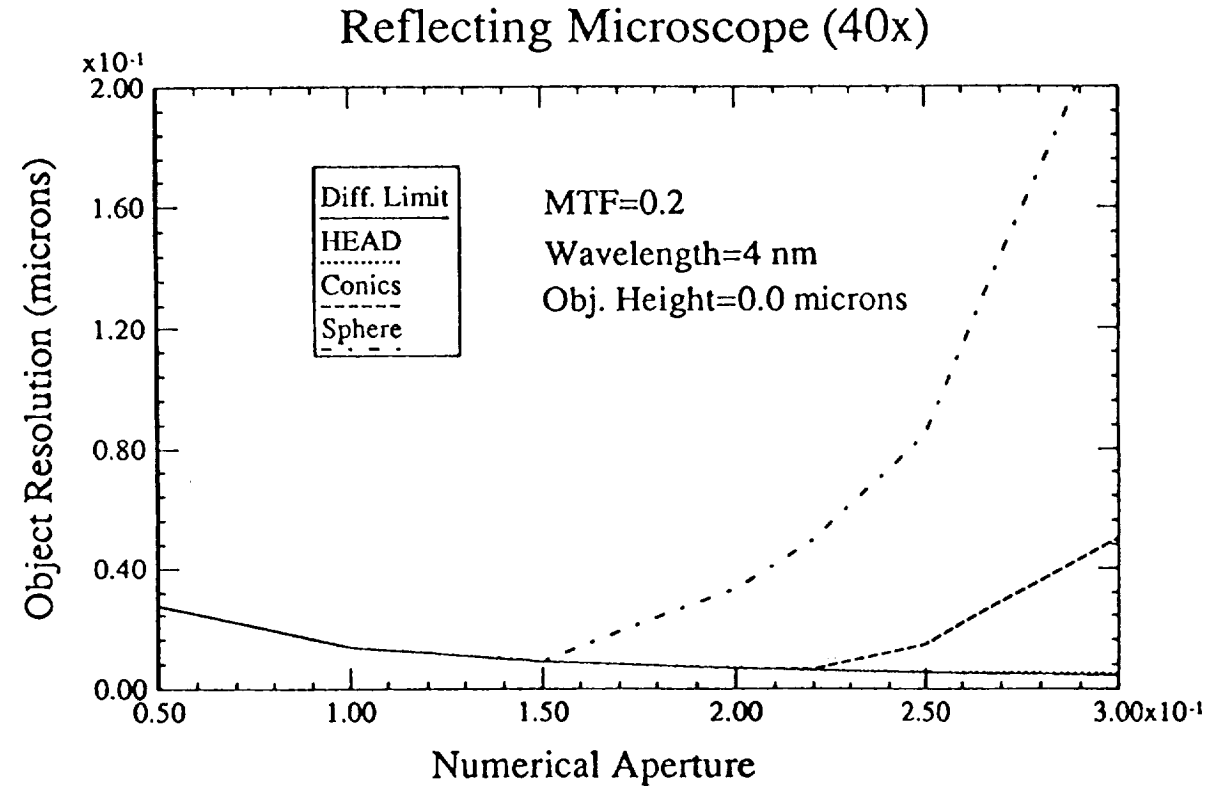

Fig. 2. Comparison of object plane resolution between spherical, conic, and Head microscopes as a function of the primary mirror NA.

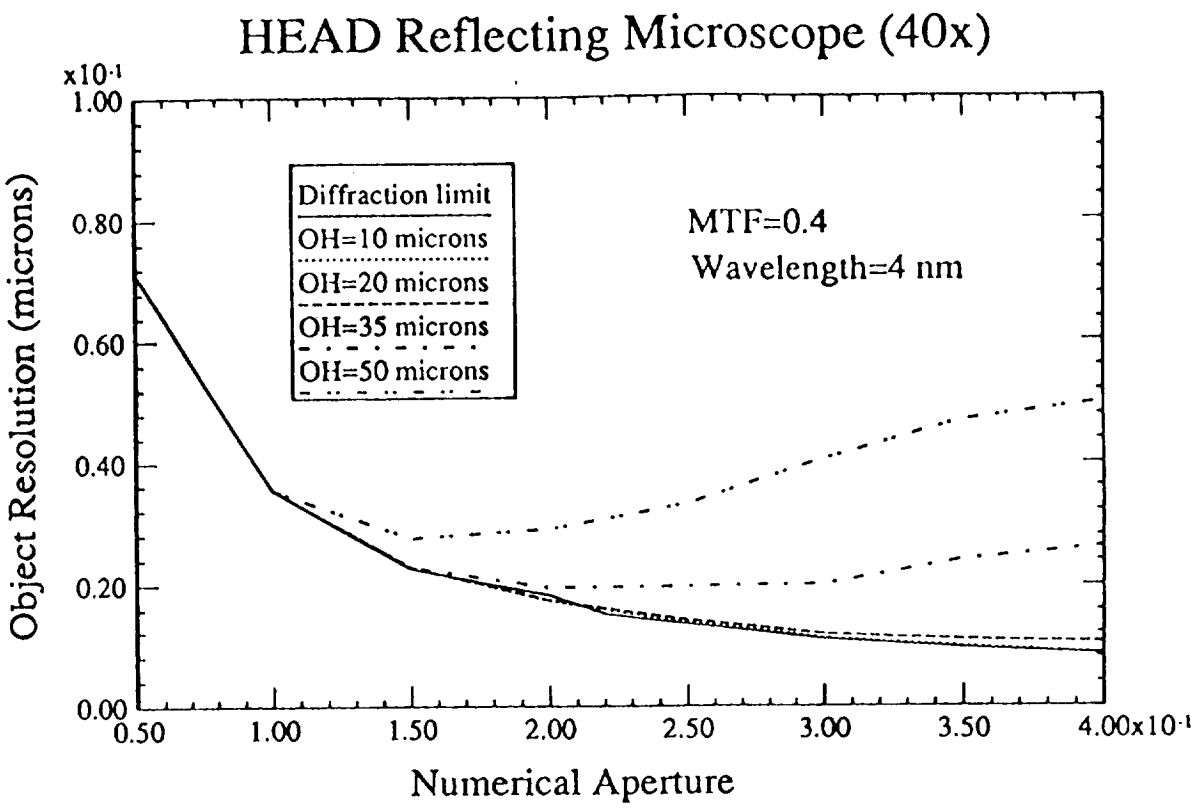

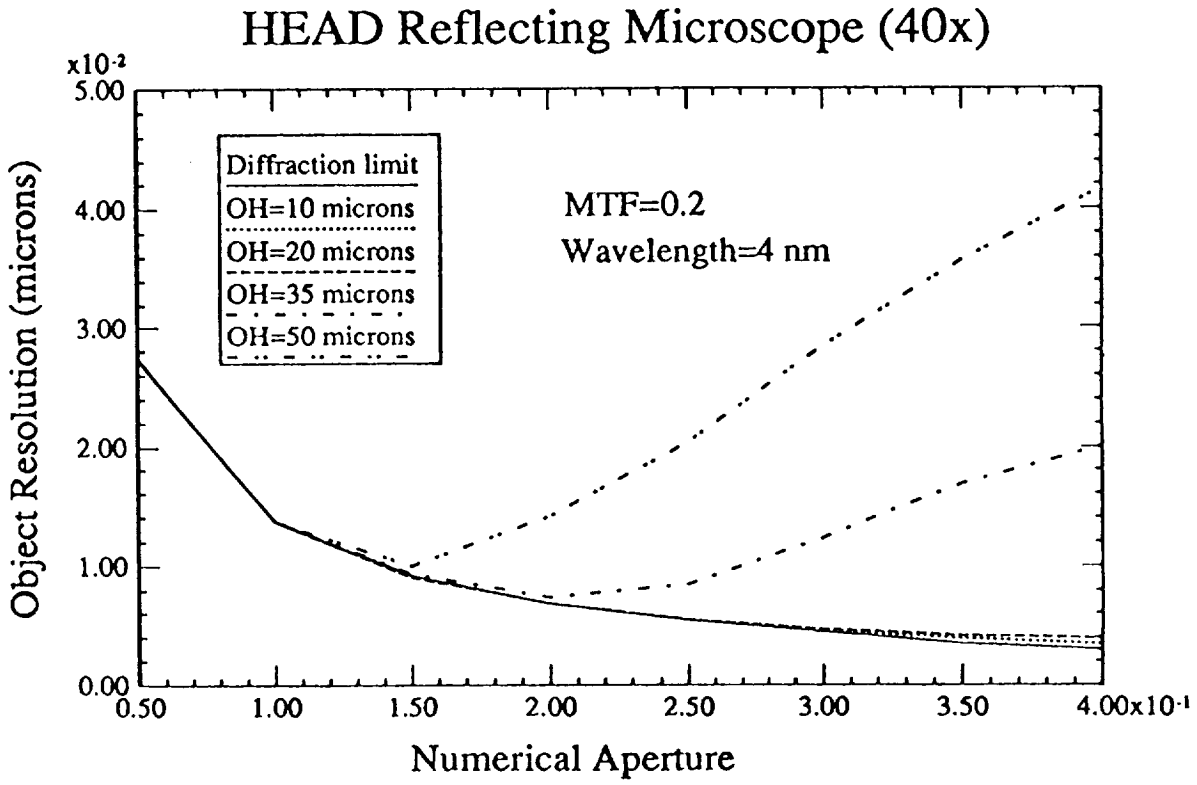

Fig. 3. Comparison of the object plane resolution for a Head microscopes as a function of the primary mirror NA for different object heights.

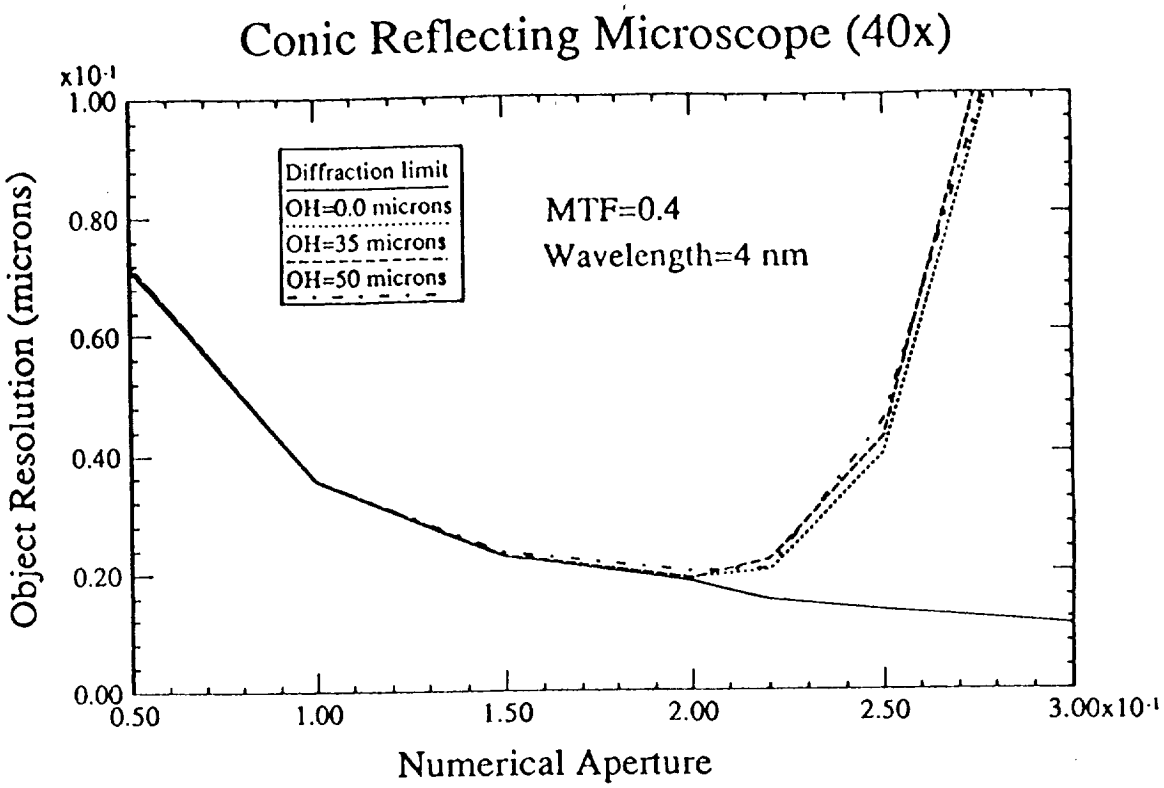

Fig. 4. Comparison of the object plane resolution for a conic microscope as a function of the primary mirror NA for different object heights.

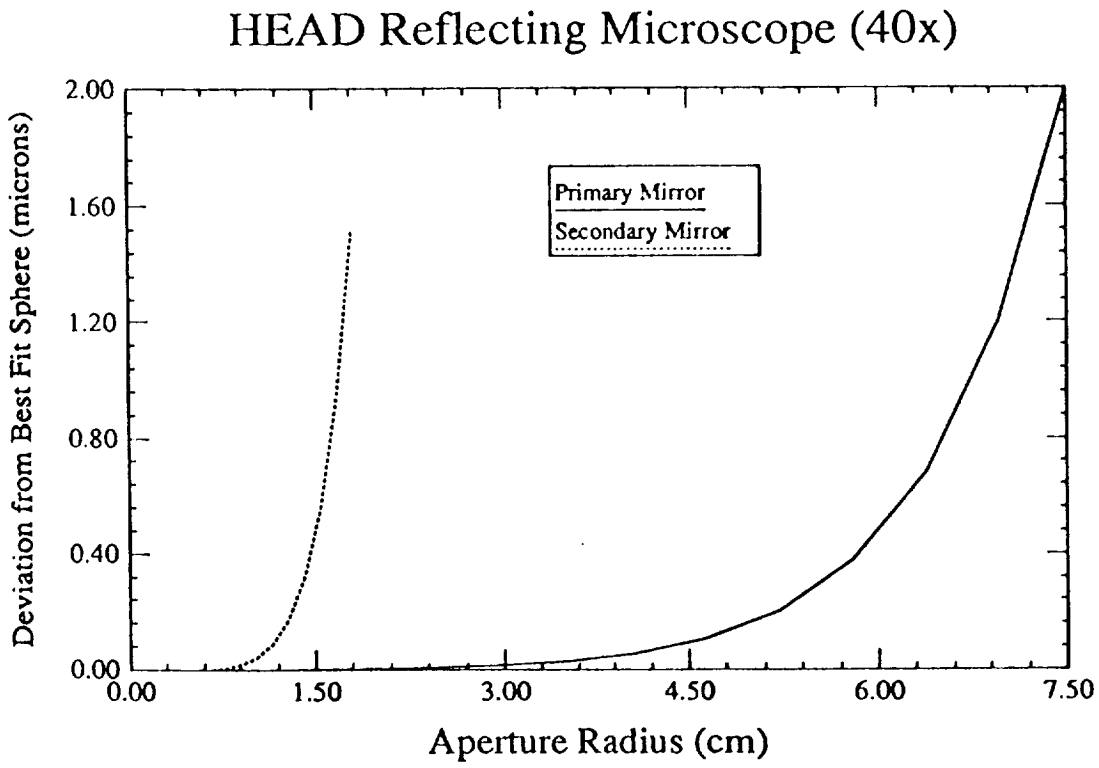

Fig. 5. Deviation of Head microscope surfaces from best fit spherical surface versus aperture radius.

For practical considerations, it is important to examine the depth of focus for the high NA and large M microscopes that have been analyzed. From diffraction theory, the depth of focus, DoF, is given by

$$DoF = \frac{\lambda}{(NA_{im})^2}. \tag{4}$$

Combining Eqs. (2) and (4) gives the following expression for the DoF

$$DoF = \frac{\lambda M^2}{(NA)^2} \tag{5}$$

where NA is the object space numerical aperture. Figure 6 presents a plot of the image plane depth of focus versus NA for different M with 100 Å radiations. From Eq. (5), it follows that the DoF varies linearly with λ. Thus, the DoF values given in Fig. 5 can be scaled linearly to the desired wavelength. For example, the depth of focus of a 40x microscope with a NA of 0.3 will be 160 microns for operations at 100 Å and 64 microns for operations at 40 Å.

3. CONCLUSIONS

This study has shown that a conic reflecting microscope with NA $\leq$ 0.22 will yield near diffraction limited performance for objects with a diameter of 100 microns. The Head reflecting microscope with NA $\leq$ 0.4 will yield near diffraction limited performance for objects with a diameter of 40 microns when operating with 40 Å radiation and should be able to resolve object features about 50 Å in size. Plans are being formulated to fabricate a water window conic microscope and a Head microscope that should be able to resolve cell features smaller than 100 Å. These microscopes would make a significant contribution to the field of x–ray microscopy of cell biology.[11]

4. ACKNOWLEDGEMENTS

The authors would like to express gratitude to the Center Director's Discretionary Fund of NASA/MSFC and to Los Alamos National Lab for partial support of this research.

5. REFERENCES

1. H. Kinoshito, K. Kurilhara, Y. Ishil, and Y. Torii, "Soft x–ray reduction lithography using multilayer mirrors," J. Vac. Soc. Techno. B7(6) 1648–1651 (1989).

2. D. L. White, J. E. Bjorkholm, J. Bokor, L. Eichner, R. R. Freeman, J. A. Gregus, T. E. Jewell, W. M. Mansfield, A. A. MacDowell, E. L. Raab, W. T. Silfvast, L. H. Szeto, D. M. Tennant, W. K. Waskiewicz, D. L. Windt, O. R. Wood, II, "Soft–x–ray projection lithography: experiments and practical printers," Proc. SPIE 1343, 204–213 (1990).

3. K. A. Tanaka, M. Kado, H. Daido, T. Yamanaka, S. Nakai, K. Yamashita, and S. Kitamoto, "Schwarzschild microscope at λ = 7 nm," in Soft–X–Ray Projection Lithography, 1991, Technical Digest Series, (Optical Society of America, Washington, DC 1991), 77–79.

4. D. L. Shealy, R. B. Hoover, A. B. C. Walker, Jr., and T. W. Barbee, Jr., "Development of a normal incidence multilayer, imaging x–ray microscope," Proc. SPIE 1160, 109–121 (1989).

5. D. L. Shealy, D. R. Gabardi, R. B. Hoover, A. B. C. Walker, Jr., J. F. Lindblom, and T. W. Walker, Jr., "Design of a normal incidence multilayer imaging x–ray microscope," J. X–Ray Sci. Techno. **1**, 190–206 (1989).

6. D. L. Shealy, R. B. Hoover, T. W. Barbee, Jr., and A. B. C. Walker, Jr., "Design and analysis of a Schwarzschild imaging multilayer x–ray microscope," Opt. Eng. 29.7, 721–727 (1990).

7. D. L. Shealy, W. Jiang, and R. B. Hoover, "Design and analysis of aspherical multilayer imaging x–ray microscope," Proc. SPIE **1343**, 122–132 (1990).

8. A. K. Head, "The two–mirror aplanat," Proc. Phys. Soc. **LXX**, 10–B, 945–949 (1957).

9. Genesee Optics Software, 20 University Avenue, Rochester, NY 14605.

10. R. A. London, M. D. Rosen, and J. E. Trebes, "Wavelength choice for soft x–ray laser holography of biological samples," Applied Optics **28.15**, 3397–3404 (1989).

11. M. R. Howells, J. Kirz, and D. Sayre, "X–ray microscopes," Sci. Am., 88–94, February, 1991.

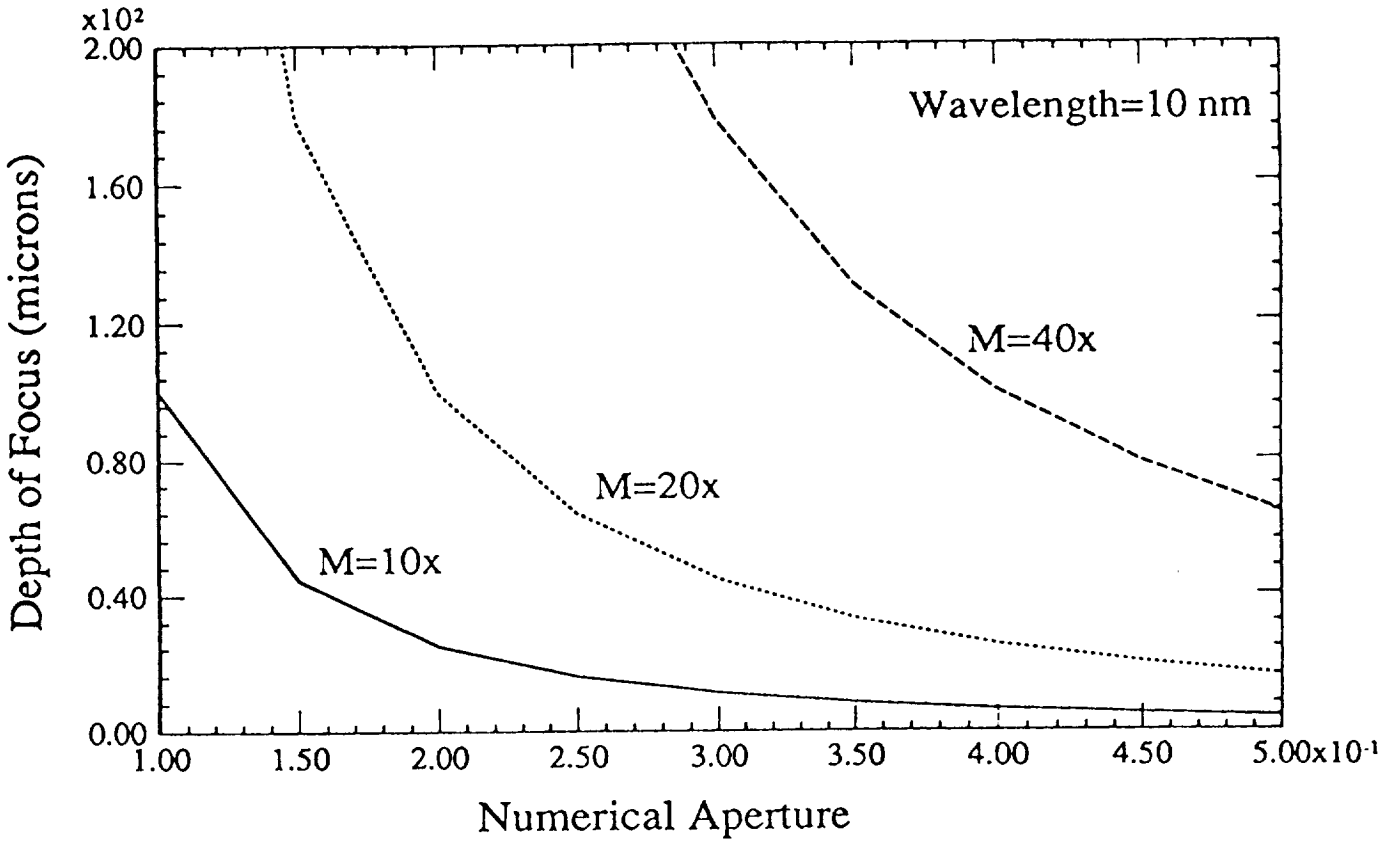

Fig. 6. Depth of focus of the image plane of a reflecting microscope versus the primary mirror NA.

Report Documentation Page

1. Report No.	2. Government Accession No.	3. Recipient's Catalog No.
Final		

4. Title and Subtitle

X-Ray Microscope Assembly and Alignment Support and Advanced X-Ray Microscope Design and Analysis

5. Report Date

October 28, 1991

6. Performing Organization Code

7. Author(s)

David L. Shealy

8. Performing Organization Report No.

10. Work Unit No.

9. Performing Organization Name and Address

Department of Physics
University of Alabama at Birmingham
1300 University Boulevard, Room 310
Birmingham, AL 35294-1170

11. Contract or Grant No

H-06853D

13. Type of Report and Period Covered

Final Report
5/10/90 - 9/30/91

12. Sponsoring Agency Name and Address

NASA/MSFC
Marshall Space Flight Center, AL 35812

14. Sponsoring Agency Code

15. Supplementary Notes

16. Abstract

Work under this contract has been focused on two tasks:

1. Advanced x-ray microscope and telescope design, and
2. Assembly and alignment support for Schwarzschild x-ray microscope.

Results obtained as part of Task 1 have been reported to NASA/MSFC PI (R.B. Hoover) and published in Optical Engineering and in the Proceedings of the SPIE. See Appendices 1-3 for reprints of the manuscripts. Work associated with task 2 involved a UAB research assistant (D. Gore) working with R.B. Hoover at NASA/MSFC on this project and developing related technical skills. However, assembly and testing of the Schwarzschild microscope is not complete and is continuing into FY 92, when experimental results are expected.

17. Key Words (Suggested by Author(s))	18. Distribution Statement
x-ray optics microscope multilayer Schwarzschild microscope Head microscope reflective optics	Available to the public

19. Security Classif. (of this report)	20. Security Classif. (of this page)	21. No. of pages	22. Price
unclassified	unclassified	28	

NASA FORM 1626 OCT 86